Estuaries and Coasts (2026) 49:53
https://doi.org/10.1007/s12237-025-01653-7

MANAGEMENT APPLICATIONS

Water Exchange Characteristics of Tidally Influenced Hydrilla Invasion Sites in the Lower Connecticut River

Andrew W. Howell[1] · Benjamin P. Sperry[2] · Jens P. Beets[3] · Michael W. Durham[2] · Jonathan S. Glueckert[4] · Amber E. Riner[5]

Received: 2 July 2025 / Revised: 14 November 2025 / Accepted: 9 December 2025

Abstract

The Lower Connecticut River (CR) is an ecologically and recreationally significant ecosystem within New England, but the river has become increasingly vulnerable to the intrusion of aquatic invasive species (AIS) like hydrilla (*Hydrilla verticillata*). The hydrilla population recently discovered in the Lower CR is genetically unlike former hydrilla clades present in the United States. The specific biological and management components of this unique clade-C hydrilla in comparison to its cohorts remains largely undetermined and the nature of management action to combat the submersed plant within the tidally influenced lotic system further complicates waterway resilience efforts due to high-water exchange. Because of the inherent environmental challenges attributed to lotic environs, the use of aquatic herbicides remains the primary management tool for selective and effective hydrilla control. However, knowledge of the site-specific water exchange processes at infested sites coupled with subspecies- and herbicide-specific concentration-exposure time (CET) requirements are essential for successful plant management. The primary goal of the present studies was to quantify bulk water exchange rates at five representative hydrilla infestation sites within the Lower CR using Rhodamine WT dye (RWT) to mimic prospective herbicide application operations. Dye monitoring indicated distinct variability among study site water exchange rates, with RWT half-lives ranging from 0.35 to 72.36 h following application. Future management efforts deploying herbicide should consider these methods and findings when selecting appropriate herbicide active ingredients and use rates to achieve hydrilla control. While the present water exchange findings offer initial guidance, comparable dye studies will be necessary as management programs target additional hydrilla invasion areas within the river.

Keywords Invasive species · Hydrilla verticillata · Rhodamine WT dye · Tidal systems · Fluvial dynamics

Introduction

The tidal influence of the Lower Connecticut River (CR), Connecticut (CT), has supported an extensive and diverse ecosystem of submersed aquatic vegetation (SAV) and associated fauna. Historically, aquatic and marsh habitats within the Lower CR have sustained an abundance of native macrophytes including *Lemna minor* L., *Elodea nuttallii* (Planch.) H. St. John, *Vallisneria americana* Michx., *Utricularia radiata* Small, and various *Potamogeton* spp. (Moore et al., 1999; CAES, 2020). Aquatic plants are highly productive and provide enumerable environmental benefits including spawning habitat, oxygenation, benthic stabilization, and physiochemical water quality functions (Moore et al., 2010). Unfortunately, these same conditions that support beneficial native macrophytes has also supported the prevalence and spread of aquatic invasive species (AIS) like

Communicated by Karen Lisa Knee

✉ Benjamin P. Sperry
Benjamin.P.Sperry@usace.army.mil

1 Department of Crop and Soil Sciences, North Carolina State University, Campus Box 7620, Raleigh, NC 27695, USA

2 Research Biologist, Army Engineer Research and Development Center, Environmental Laboratory, Gainesville, FL, USA

3 Research Ecologist, Department of Agriculture, Agricultural Research Service, Invasive Species and Pollinator Health Unit, Davis, CA, USA

4 Biologist, University of Florida Center for Aquatic and Invasive Plants, Gainesville, FL, USA

5 Oak Ridge Institute for Science and Education Intern and Graduate Student, University of Florida Center for Aquatic and Invasive Plants, Gainesville, FL, USA

Published online: 27 January 2026

hydrilla (*Hydrilla verticillata* L.f. Royle) which, readily displace natives (flora and fauna) and restricts a water's utility (Langeland, 1996; Madsen & Sand-Jensen, 1991; Smart et al., 1994; Zhang & Boyle, 2010).

Hydrilla has been referred to as the "perfect aquatic weed" and has successfully invaded countless waterways throughout the United States (US) (Langeland, 1996; Jacono et al., 2025). Previously, only two genetically distinct biotypes of hydrilla were recognized in the US. The dioecious biotype which spread from Florida (FL) and Georgia (GA) to Texas following discovery in the 1950 s (Steward et al., 1984; Netherland, 1997), and monoecious hydrilla which rapidly established in cooler climates from central GA to CT westward following discovery in Maryland (MD), Delaware, and North Carolina (NC) in the 1980 s (Haller, 1982; Steward et al., 1984; Schmitz et al., 1991). Most recently in 2020, a third genetically distinct strain (clade-C) was confirmed in the Lower CR, which presents unique morphological characteristics and potentially unique management challenges (Tippery et al., 2020; Foley et al., 2024).

Hydrilla primarily spreads via fragmentation and vegetative propagules (axillary and subterranean turions). Seasonal turion production not only serves as a means of plant establishment and spread, but also as a form of overwintering for succession (Netherland, 1997; True-Meadows et al., 2016). There are known biological and phenological differences between monoecious and dioecious hydrilla including timing and quantity of vegetative propagule production, timing of biomass production, and flowering (True-Meadows et al., 2016). Anecdotal reports indicate clade-C hydrilla also has distinctive biological characteristics including turion production and self-abscission (Tippery et al., 2020; Foley et al., 2024; Beets, 2024). Regardless of the clade, hydrilla infestations in lotic systems have remained far less studied than infestations in lentic environments. Tidal and high-flow systems such as the Lower CR may also contribute to increased hydrilla dispersal via propagule and stem-fragment hydrochory.

Invasive species such as hydrilla can negatively impact the ecosystem and hydrology of impacted waterways. Hydrilla can rapidly reestablish following environmental stresses or management from vegetative propagules (Langeland, 1996). The submersed plant also has rapid growth rates, a low light compensation point, salinity tolerance (up to 7 ppt), and C4-like photosynthesis which improves its competitive ability compared to many native macrophytes (Langeland, 1996; True-Meadows et al., 2016). While hydrilla infestations may fill empty ecological niches in some aquatic systems, dense infestations ultimately decrease fish length, species richness, native vegetation, and generally degrades the water's habitat (Schultz and Dibble, 2012; Hoyer et al., 2008; Hofstra and Clayton 2014; Londe et al., 2024). Hydrilla and other invasive submersed aquatic vegetation can act as ecosystem engineers, redirecting and reducing water flow, and negatively impact hydropower, navigation, and recreation (Jones et al., 1997; True-Meadows, 2016; Santos et al.,2011; Hofstra et al., 2010). In the Lower CR, hydrilla invasion has potential to destructively alter breeding habitats of critically endangered anadromous species like Atlantic Sturgeon (*Acipenser oxyrinchus*) (Savoy et al., 2017; NMFS, 2024). Therefore, hydrilla management is essential to steward critical water resources like those of the Lower CR.

Several management opportunities exist to combat the deleterious effects of invasive SAV like hydrilla. Mechanical (e.g., cutting or suction harvesting), physical (e.g., benthic barriers), and biological (e.g., grass carp [*Ctenopharyngodon idella*]) all provide varying levels of success in lentic environs (Sutton, 1977; Haller et al., 1980; True-Meadows et al., 2016). However, these management approaches are complicated or are not feasible in riverine settings due to ecological, regulatory, and cultural restrictions, and do not provide the appropriate mechanisms required to effectively control hydrilla in a settings like the Lower CR. Therefore, the most environmentally sound and effective management programs in lotic systems often include the use of aquatic herbicides to selectively target AIS. Still, the use of aquatic herbicides for in-water settings is complex and requires sound knowledge of treatment depth, breadth, and water exchange rates to ensure proper dosing of chemical applications.

Herbicide concentration-exposure time (CET) relationships are a key concept in the chemical management of submersed aquatic weeds. This relationship consists of herbicide concentration in contact with plants and the length of time the herbicide remains in the target area surrounding the plant (Netherland & Getsinger, 1992). Simply put, as water exchange rate increases, herbicide CET decreases. The CET requirements for effective control are unique to different plant species, plant size and density, and the herbicide used. When properly understood, plant-herbicide CET relationships can be used to tailor herbicide applications by reducing herbicide inputs into aquatic systems and provide targeted selectivity, thus decreasing the potential for non-target damage to desirable or protected plant species (Getsinger & Netherland, 2018). An accepted method for measuring and modeling site-specific CET involves the use of fluorescent tracer dyes to measure bulk water exchanges. Since the 1980 s, dyes such as rhodamine water tracing (RWT), have been used as inert surrogates to mimic and quantify herbicide dispersion and improve the holistic understanding of hydrodynamic systems (Fox & Haller, 1992; Turner et al., 1994; Sartain et al., 2023; Getsinger et al., 2024). Rhodamine WT dye is most utilized due to its

favorable toxicity profile, ease of detection, high correlation with aquatic herbicides, and approval for use in potable water at concentrations up to 10 µg L^{-1} (Getsinger et al., 2024). Tracer dyes, particularly RWT, are regularly used to understand flow dynamics including wetland flows, groundwater tracing, river hydrodynamics, transient storage, and piscicide tracking (Williams & Nelson, 2011; Runkel, 2015; Zhu et al., 2017). While RWT dye applications are most commonly used to determine bulk water exchange, this dye has been correlated with the aquatic herbicide triclopyr, with no significant difference between dye and herbicide half-lives (Turner et al., 1994).

The Lower CR inherently poses greater fluvial complexity than that of non-tidally influenced inland river systems. For example, unlike inland rivers or run-of-the-river reservoirs with unidirectional flows (Sartain et al., 2022; Wersal et al., 2022), the Lower CR experiences flows downstream and upstream (flow reversal) dependent upon the tide cycle. These bidirectional flows are thus a major factor affecting flow consistency, water levels and flooding, chemical (e.g., salinity) and physical (e.g., turbidity) water quality, and ultimately hydrilla management strategies using herbicide in the system (Weiss et al., 1982; Fox et al., 1991a, b; Whitney et al., 2021). Prior RWT dye studies in Crystal River, FL characterized bulk water exchange patterns based upon tidal cycle and seasonality, SAV density, and water temperature to provide enhanced operational hydrilla management guidance with herbicide (Fox et al., 1991a, b; Fox & Haller, 1992); however, these dead-end canal systems studied were of smaller origin (420 m long) than the Lower CR (approx. 56 km long) and were spring-fed influenced which limits comparative utility. Another RWT dye study in the Potomac River, MD/VA found the presence of densely dominated hydrilla beds effected tidal flow through frictional forces, where hydrilla stands appeared more uniformly penetrable and more spatially homogenous during ebb cycles (Rybicki et al., 1997). While the aforementioned studies provide some initial insight into possible hydrodynamic patterns associated with hydrilla infested tidal river systems, bulk water exchange processes are unique among, and within, flowing water systems (Getsinger & Netherland, 2018). Therefore, conducting discrete dye studies is necessary to link CET relationships with water exchange evaluations to aid in predicting herbicide effectiveness (formulation and delivery methods), meet regulatory expectations (state and federal), and to select treatment sites where AIS control is most likely to succeed in the Lower CR.

Due to the complex fluvial dynamics of the Lower CR, the specific objectives of this study were to:

(1) characterize water exchange patterns in five geographically and tidally distinct hydrilla-invaded sites to evaluate the influence of tide cycle in relation to measured bulk water exchange patterns, and.

(2) model the relative bulk water exchange half-lives of select sites to guide future understanding of herbicide CET requirements for effective hydrilla management.

While the present study provides initial guidance for the chemical management of hydrilla and other potentially noxious AIS, this work also contributes to the broader understanding of site-specific bulk water exchange patterns in tidally influenced rivers. For example, the specific fluvial dynamics and associated influences measured could also be used for understanding water quality patterns or potential anthropogenic disturbance modeling components (e.g., nutrient exchange rates and harmful algal blooms).

Materials and Methods

Study Site Description

Connecticut River System

The Lower CR (Fig. 1) is the longest tidal waterway (653 km) in the New England region of the United States (US). The river forms south (270 m) of the Canadian border at the Fourth Connecticut Lake, New Hampshire (NH; 45.247707°N, 71.214018°W) and continues southward through four US states (Vermont (VT), NH, Massachusetts (MA), and Connecticut (CT), respectively) until discharging in the Long Island Sound estuary. The CT portion of the Lower CR meanders approx. 109 km (bisecting the middle of the state) and supports a 2,719 km^2 watershed that provides critical environmental, agricultural, residential, and recreational opportunities (Clay et al., 2006). Water quality records from Old Lyme, CT (01194796; closest monitoring station to the estuary) from the past two decades indicate prominent climatic variation patterns of water temperature (−0.3 to 29.1 °C), conductivity (77 to 48,300 µS), and salinity (0 to 31 PSU) within the Lower CR tidal system depending on seasonality (USGS, 2024). Though seasonal water velocities are not well defined due to current sparsity in monitoring stations along the Lower CR, average peak annual discharge is estimated with a mean of 2292 m^3s^{-1} based upon river velocity values reported at Middle Haddam, CT (01193050) and Hartford, CT (01190070) monitoring stations (USGS, 2024).

Tidal currents within the Lower CR are semidiurnal and can appear moderately stochastic based upon sampling location along the river due to bathymetric variation, lunar

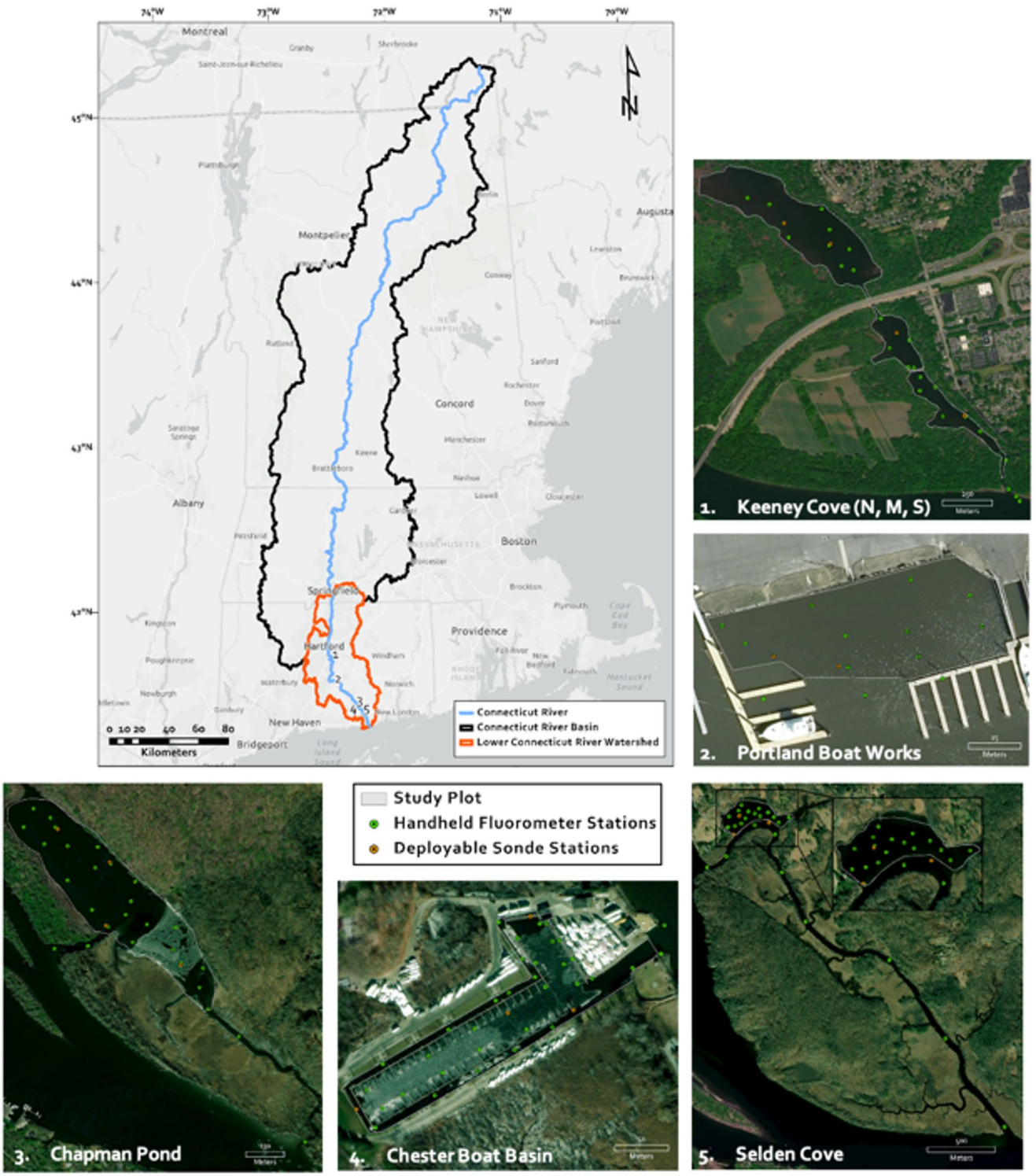

Fig. 1 Map depicting study site locations within the Lower Connecticut River and the associated rhodamine (RWT) dye sampling stations (handheld and deployable sondes) within site plots to monitor bulk water exchange patterns due to discrete ecological parameters and tidal influences

seasonality, river discharge, and climatic conditions (Parker, 2007). Stephens et al., 1963) noted that the presence of vegetation further affects water exchange cycles within flowing water systems like the Lower CR. Since tidal cycles are predictable periodic phenomenon (Parker, 2007), the Lower CR is an excellent candidate to study the influence of tidal interactions and the associated water exchange patterns within select hydrilla infested sites.

Specific study sites were defined using aquatic vegetation survey data collected in fall 2019 by the Connecticut Agricultural Experiment Station (CAES, 2020). These initial data provided relevant aquatic plant density and distribution estimates to define suitable study plots (e.g., augmented coves, ponds, marinas, or creeks) adjacent to the main Lower CR channel. Generally speaking, this river channel has a relatively high flow rate (>28 m^3s^{-1}), and experiences tidally influenced water exchange cycles. To ensure the pilot study sites were appropriate for monitoring bulk water exchange, treatment plots within identified sites were selected when hydrilla was documented as the dominant SAV within the CAES Invasive Aquatic Plant Program (IAPP) surveyed area.

Treatment Plot Descriptions

Five geographically distinct study plots, invaded with hydrilla, were selected to evaluate water exchange characteristics in the Lower CR system. Each study plot represented a unique location along the Lower CR based upon locational proximity (e.g., tributary, marinas, and public boating access) and aquatic weed abundance. Selected plots represented 51 river km of the Lower CR from Keeney Cove (41.723325°N, 72.630372°W; Glastonbury, CT) to Selden Cove (41.411311°N, 72.416219°W; Lyme, CT). Individual plot descriptions and locations along the Lower CR and associated physical and ecological parameters are provided in Table 1 and (Fig. 1).

Bathymetry measures, Tidal corrections, and Water Volume Calculations

Initial study site evaluations were conducted spring 2023 to provide bathymetric reference and calculate designated plot water volumes. The U.S. Army Corps of Engineers (USACE) New England District (NAE) utilized shallow water sampling and survey operation protocols to conduct initial hydrographic surveys (USACE 2013). Survey vessel positioning was achieved using a Hemisphere Vector VS330™ (Hemisphere GNSS, Scottsdale, AZ, USA) Real Time Kinematic (RTK) position and heading system interfaced to a laptop computer with Hypack® (Xylem, Washington, DC, USA) survey software. Locational corrections were accessed from the University of Connecticut's Advanced Continuously Operating Reference Network (ACORN) to update spatial positioning data in real-time via cellular connection. Tidal corrections were conducted in Hypack® software by applying local tide model offsets from the National Oceanic and Atmospheric Administration (NOAA) Vertical Datum Transformation (VDatum) tool to the RTK orthometric (mean sea level) recordings whilst in-field. Water column depth measurements occurred with a single beam hydroacoustic sensor and CEESCOPE echosounder (CEE HydroSystems USA, Carlsbad, CA, USA) having a 200 kHz, 9° transducer operating at a 20 Hz ping rate affixed to a vertically adjustable survey boom. Water column measurements at respective study sites included conductivity and temperature depth profiles (i.e., CTD profiles) with a SonTek Castaway®–CTD (YSI, Yellow Springs, OH, USA) during these initial evaluations. Depth profiles were uploaded to the Hypack® software to correct water column sounding variations. The resultant hydroacoustic datasets were post-processed in Hypack® SBMAX64. Shapefiles containing for each study site were then exported to ArcMap (ESRI, Redlands, CA, USA) where Triangular Irregular Network (TIN) bathymetric surfaces were created using study plot data in conjunction with shoreline LiDaR contours collected from Connecticut's Capitol Region Council of Government (CRCOG) 2016 statewide survey (https://gis.crcog.org/p

Table 1 Site-specific vegetation and tidal parameters of the five study sites selected for water exchange evaluations

Study plots[a]		Surface area (ha)		Mean tide (m)[c]		Calculated volume (m^3)[d]	
	Aquatic vegetation[b]	Low tide	High tide	Low tide	High tide	Low tide	High tide
Keeney Cove							
South	Hv	2.11	4.53	--	--	19,418	36,208
Middle	Hv	2.97	3.98	--	--	27,522	46,303
North	Hv, Tn	2.11	18.60	--	--	25,835	94,380
Total		7.19	27.11	0.04	0.59	72,774	176,890
Portland Boat Works	Hv	0.08	0.16	0.02	0.72	186	1,092
Chapman Pond	Cd, Hv, Va, Tn	20.22	26.78	0.03	0.90	267,732	467,677
Chester Boat Basin	Hv	1.48	1.78	0.04	0.93	20,730	35,041
Selden Cove	Hv, Ec	6.10	6.56	0.04	0.96	24,856	84,527

[a]Keeney Cove was split into three plots: South (south of Point Rd. bridge to main river channel), Middle (south of CT Rt. 3 bridge), and North (north of CT Rt. 3 bridge)

[b]Aquatic vegetation recorded during plot pre-treatment assessments: *Hydrilla verticillata* (Hv); *Trapa natans* (Tn); *Vallisneria americana* (Va); *Ceratophyllum demersum* (Cd); *Elodea canadensis* (Ec)

[c]Mean low water (MLW) represents the average low tide, while mean high water (MHW) represents the average high tide inundation

[d]Site-specific water volumes were calculated using in situ real-time kinematic positioning water level corrections and tidal predictions

ortal/apps/sites/#/crcog-portal-site). Water volumes were calculated for each study site using the TIN surface and a reference plane informed from RTK water level corrections at the respective times of each site-specific bathymetric survey.

Dye Application and Monitoring

Liquid RWT dye (20% Rhodamine WT, KeyColour Inc., Phoenix, AZ, USA) was applied to the selected Lower CR plots using an outboard vessel or airboat equipped with a 378 L spray tank and six weighted-drop hoses, which trailed behind the vessel. Drop hoses were affixed to the vessel's stern such that the applied dye solutions were equivalently discharged 30 to 40 cm below the water's surface to mimic common herbicide application techniques. The RWT treatment targeted an in-water dye concentration of 10 µg L^{-1} using calculated water volumes and plot dimensions determined at low tide conditions (Table 2). Dye applications were delivered through densely infested hydrilla plots to simulate an operational aquatic herbicide treatment.

Prior to RWT dye application, a water sample from each discrete site was collected from the respective treatment plot to serve as liquid carrier used for calibrating all fluorometry equipment. For this study, it was critical to obtain site-specific water due to the likely changes in water quality (i.e., turbidity) based on study site proximity along the river which could ultimately influence subsequent field-collected dye readings due to inherent variation in water clarity. All fluorometry equipment was calibrated using a four-point calibration (0, 1, 10, and 25 µg L^{-1}).

Immediately following dye application at each site, water column RWT dye measurements ensued from a vessel at preselected georeferenced sampling points. Depending upon the bathymetric contours and overall size of the treatment plot, samples were measured and logged at ≥10 points within, and ≥2 points directly outside (Figs. S1-S5), the treatment plots using a handheld Cyclops-7 submersible fluorometer (Turner Designs, Sunnyvale, CA, USA). Handheld measurements occurred at 0.15 m below the water's surface (surface), mid-water column (middle), and 0.15 m above the sediment (bottom) at each discrete sampling point. When water column depths were >3 m at a given sample point, additional water column measurements were recorded at 1 m intervals in-between the surface, middle, and bottom measurements. Handheld RWT half-life measurements took place at 4 to 6 h intervals following initial dye applications, with measurements continuing until whole-plot readings dissipated to ≤1.0 µg L^{-1} RWT. Depending upon site and weather conditions, if the 1.0 µg L^{-1} RWT detection was not achieved by 72 to 170 h after treatment (HAT), measurements were concluded due to equipment and personnel obligations with additional study sites. In addition to handheld measurements, continuous recordings occurred with deployable data sondes (N=4 per site; Hydrolab HL4 Sonde, Ott HydroMet, Kempten, Germany) set to capture dye concentrations and water quality metrics [turbidity Formazin Nephelometric Unit (FNU), temperature (°C), dissolved oxygen (mg L^{-1}), and pH)] at 15 min intervals. Deployable data sondes were placed systematically (e.g., near inlet or outlet locations; among areas with dense, or devoid of, vegetation) at 1.0 m below the water's surface within respective treatment plots using anchored buoys (Figs. S1 to S5). The deployable sondes functioned as intertidal monitoring stations used to assess environmental variation (e.g., diurnal patterns and vegetation biovolume due to receding tide) which could lead to dye gradient extremes (i.e., dye concentration endpoints) as influenced by unique water exchange patterns (i.e., tidal flow and direction). Deployable sondes were removed from treatment sites upon handheld fluorometer RWT readings completion (RWT dye concentration≤1.0 µg L^{-1}).

Table 2 Site specific application parameters used for the five study sites selected for water exchange evaluations at treatment

Study plots[a]	Study plot and application metrics			
	Water level (m MLLW)[b]	Surface area (ha)	Water volume (m^3)[c]	RWT dye applied (L)[d]
Keeney Cove				
South	1.52	8.8	96,952	3.79
Middle	1.52	5.8	91,648	3.79
North	1.52	31.1	337,357	13.63
Portland Boat Works	0.91	0.2	1,480	0.08
Chapman Pond	0.91	27.0	471,189	18.93
Chester Boat Basin	0.91	1.8	34,784	1.51
Selden Cove	0.91	6.6	81,533	3.41

[a]Keeney Cove was split into three plots: South (south of Point Rd. bridge to main river channel), Middle (south of CT Rt. 3 bridge), and North (north of CT Rt. 3 bridge)

[b]Mean Lower Low Water (MLLW)

[c]Water volume used to calculate rhodamine WT dye required using MLLW and surface area measures

[d]Rhodamine WT dye applications targeted an in-water concentration of 10 µg L^{-1}. A volume calculation error led to an over application of dye at Chester Boat Basin, resulting in an initial plot concentration of 24 µg L^{-1}; however, corrected water and dye volumes are presented

Data Analysis

Resultant RWT dye measurements from each treatment plot were independently analyzed to evaluate water exchange dynamics unique to each specific study site along the Lower CR. Initial RWT dye concentrations were determined using the average measured dye applied within respective plots

following treatment (0 to 3 HAT). Only variances in the rate of dye dilution and dissipation within plots were of interest to develop water exchange patterns and evaluate RWT half-lives for the study plots. Within plots, the handheld fluorometer and deployable sonde data were separately analyzed due to the inherent differences in the measurement methods (e.g., depth of sensor readings).

For each respective recording by site, inside plot handheld fluorometer data were analyzed based upon the vertical gradient position (i.e., surface, middle, and bottom) to evaluate RWT dye distribution and dissipation within in the water column over time. However, whole plot average RWT values of the entire water column were analyzed to model actual volumetric dye dissipation rates and provide a realistic measurement of site-specific water exchange dynamics due to factors of vegetation density, tidal interaction, and bathymetric complexities. Dye half-lives calculated from whole plots further allows water exchange rates to be most readily compared between application sites (Fox & Haller, 1992). All handheld RWT dissipation data were subjected to nonlinear regression modeling using SigmaPlot software (SigmaPlot v. 14.0.3.192, Systat Software, Point Richmond, CA, USA) to establish RWT half-lives (50% initial RWT concentration measured over time). Apart from the three Keeney Cove plots, a two-parameter exponential decay equation [f=a*exp(-b*x)] was selected for dye dissipation measures where, "a" represents the initial value, "b" is the decay constant, and "x" represents time. At Keeney Cove, a three-parameter exponential decay model [f=$y0$+a*exp(-b*x)] was selected to meet model assumptions of normality and Spearman Rank, and to best capture the heightened variability in bulk water exchange patterns where "$y0$" represents the asymptotic value, "a" represents the initial value, "b" is the decay constant, and "x" represents time. To evaluate the time of vertical water column RWT dye equilibration and proportional distribution, differences in top and bottom RWT concentrations within plots were subjected to Student's t-test ($\alpha = 0.05$). Spatial interpolation of horizontal dye dissipation data was conducted using an Ordinary Kriging function in ArcGIS Pro v. 3.2.0 (ESRI Inc., Redlands, CA). A kriging interpolation method was selected due to sampling frequency and the inherent autocorrelation of data collected within RWT treatment plots (Sartain et al., 2023).

Results

Site-specific tidal dynamics, vegetation composition, and RWT dye application parameters are provided in geographical descending order along the CR flow direction (southing) in Tables 1, 2 and 3. Visual reference of study plot locale and sampling point attributes for each water exchange evaluation site are shown in (Fig. 1). Due to the wide variation in location, environmental, and volumetric factors influencing water exchange at each evaluation site, study plot results are described independently. Although treatments targeted an incoming tide, the initial dye concentration of 10 µg L^{-1} did not always occur as intended; however, the actual dye concentration achieved within plots at treatment was not compulsory to meet research objectives since the rate of half-life decay remains consistent regardless of initial concentration.

Keeney Cove

North Plot

Rhodamine WT dye measurements collected from handheld readings ($N = 10$) in Keeney Cove North at 3 HAT yielded a whole plot concentration mean of 13.7 µg L^{-1}, which was close to the target concentration of 10 µg L^{-1} [standard error (SE) ± 3.36 µg L^{-1}] (Fig. 2a). Dye measurements had vertically equilibrated by 3 HAT with no difference

Table 3 Site-specific treatment and water quality parameters for the five study sites selected for water exchange evaluations

Study plots[a]	Treatment application		Water quality and flow[b]			
	Start time	Duration (min)	Temperature (°C)	DO (mg L^{-1})	pH	Turbidity (FNU)[c]
Keeney Cove						
South	08/09/23 09:10	30	21.90	2.02	6.60	9.31
Middle	08/09/23 08:15	25	21.69	1.01	9.66	2.75
North	08/09/23 06:45	65	21.36	1.15	6.46	80.07
Portland Boat Works	09/06/23 06:20	14	24.42	8.69	7.37	1.41
Chapman Pond	08/15/23 10:20	85	23.65	8.08	8.33	1.14
Chester Boat Basin	08/22/23 15:40	23	23.55	9.26	8.19	1.97
Selden Cove	08/29/23 10:15	45	22.83	8.48	7.26	2.51

[a]Keeney Cove was split into three plots: South (south of Point Rd. bridge to main river channel), Middle (south of CT Rt. 3 bridge), and North (north of CT Rt. 3 bridge)

[b]Mean water quality values measured using deployable sonde recordings

[c]Formazin Nephelometric Unit (FNU)

[d]Flow data was collected using a handheld water flow probe

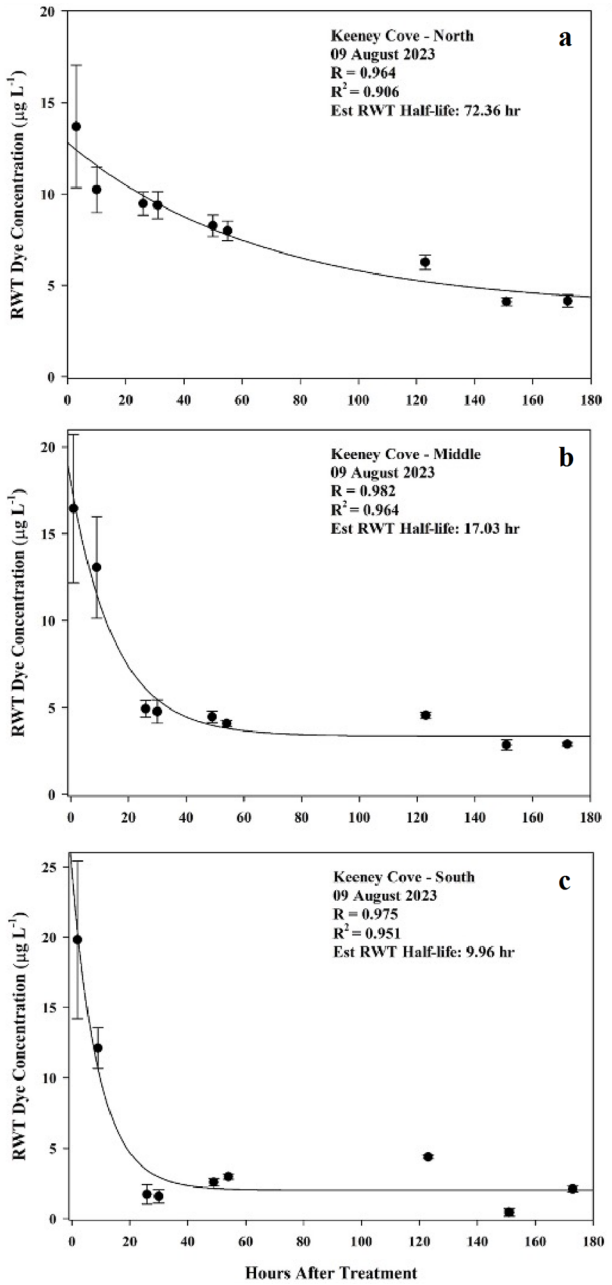

Fig. 2 Rhodamine (RWT) dye concentrations within the Keeney Cove study plots (**a**=North; **b**=Middle; and **c**=South) over time measured with a handheld fluorometer. Data points represent the mean water column RWT concentrations (±standard error) for each measured time point. Half-lives estimated using the exponential decay model, f=y0+a*exp(-b*x)

detected between surface and bottom measures until 55 HAT (P=0.028), 123 HAT (P=0.01), 151 (P<0.001), and 172 (P<0.001), according to Student's t-test (α=0.05) (Fig. 3a). Rhodamine WT dye concentration variations measured between the surface and bottom readings were proportionally nominal (2 to 2.5 µg L^{-1} higher on surface) at each evaluation period (Fig. 3a), and the reasoning in variation between surface and bottom measurements at >55 HAT is largely unknown since water temperatures appeared isothermal. The estimated RWT dye half-life within the north plot was very long (72.4 h) compared to the other Keeney Cove plots (4.3 and 7.3X longer than the Middle and South plots, respectively) (Fig. 2a). However, distinct tidal influences were detectable with the deployable sondes (N=2) as indicated by a surge (intermittent pulsing) pattern in the collected dataset (Fig S6). During these prominent tidal phases, the RWT concentration fluctuated with an amplitude up to 4 µg L^{-1} from average concentration between cycles. The RWT dye concentration at 72 HAT was 8.33 µg L^{-1} collected from data sondes, which aligns closely to the calculated whole plot half-life concentration of 6.85 µg L^{-1} with the handheld fluorometer. The minute difference between the handled and deployable fluorometers suggests both methods were capturing similar tidally influenced water exchange data in the mostly stagnate North plot. Since the dissipation rate was slow in Keeney Cove North, the study was concluded at 172 HAT with the dye still lingering at 4.14 µg L^{-1} in the North plot at conclusion. Confirmation of RWT dye residence is visually apparent in the interpolated maps (Fig. 4), where the concentration of dye persisted highest in the centralized portion of the North plot at 3 to 172 HAT.

Middle Plot

The initial whole plot RWT dye concentration collected from the handheld fluorometer (N=6) in Keeney Cove Middle at 1 HAT was 16.45 ± SE 4.28 µg L^{-1} (Fig. 2b). However, by 9 HAT the measured RWT concentration (13.06 ± SE 2.94 µg L^{-1}) more closely corresponded to the target concentration of 10 µg L^{-1}. Dye measurements within the plot had vertically equilibrated within 1 HAT with no difference detected between surface and bottom measures at any of the evaluation time points (P>0.05) which, suggests mixing within the plot happened almost immediately following the dye application (Fig. 3b). Still, the estimated half-life was relatively long at 17.03 h (8.23 µg L^{-1}) but was 55.4 h less than the estimated half-life at the Keeney Cove North plot (Fig. 2). The dye dissipation mapping indicates the highest RWT dye concentration was retained in the western portion of the plot over time (Fig. 5), which is supported by the increased density of plant material within the plot (Table 1). The deployable sonde (N=1) was located within the creek channel of the middle plot (Fig. S6) and generally displayed greater variation in dye measurements as compared to the whole plot measures made with the hand fluorometer (Fig. 2). Nevertheless, the measured dye concentrations between both RWT measurement methods showed generally similar concentration trends over the study period. Between the

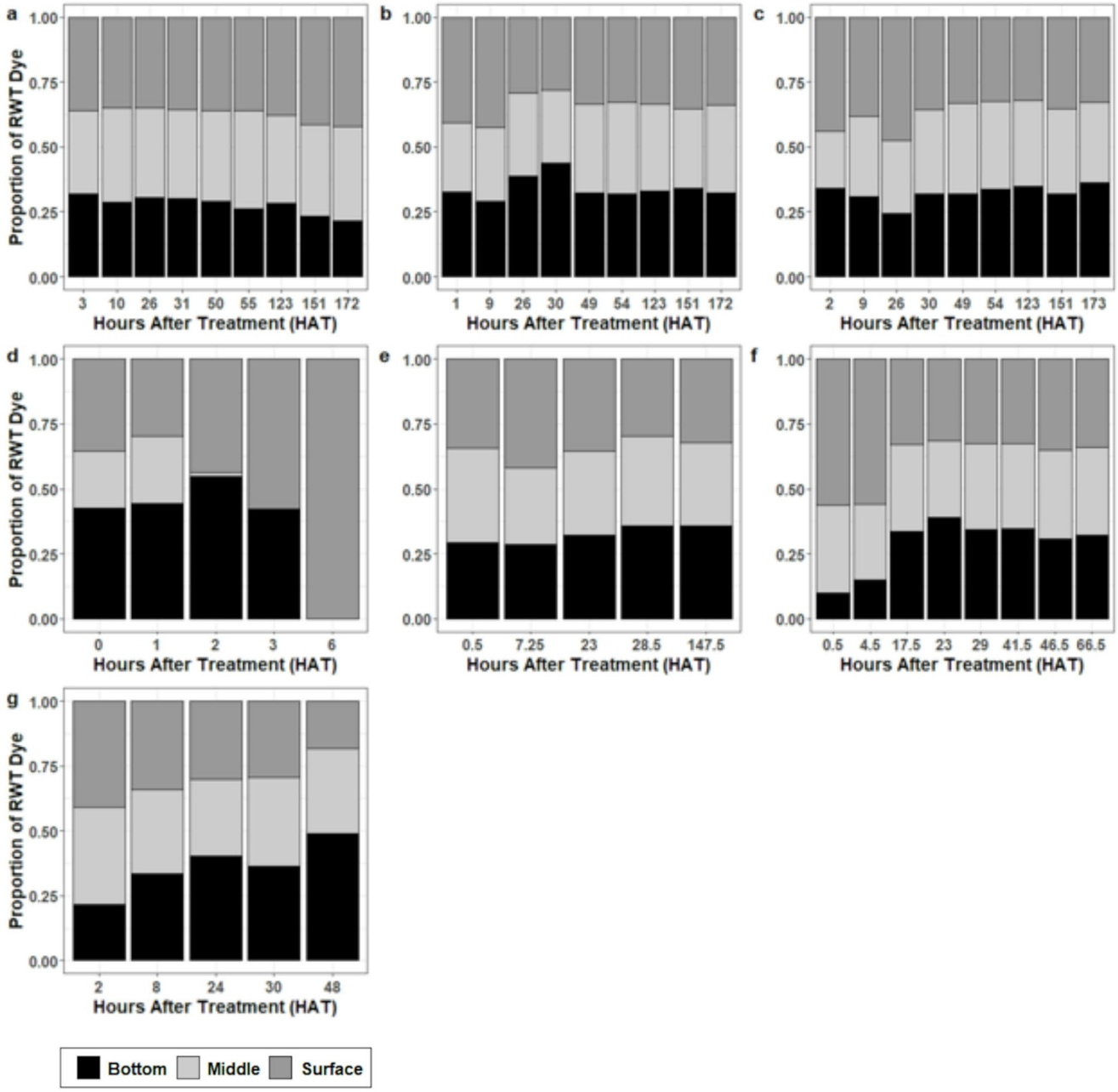

Fig. 3 Water column proportions of applied Rhodamine (RWT) dye concentrations measured using discrete handheld fluorometer samplings to evaluate the distribution (bottom, middle, or surface sample) and vertical persistence of remaining RWT dye within each study plot water column, where: **a**=Keeney Cove North; b=Keeney Cove Middle; **c**=Keeney Cove South; **d**=Portland Boat Works; **e**=Chapman Pond; **f**=Chester Boat Basin; and **g**=Selden Cove

26 HAT handheld sampling to the study conclusion at 172 HAT, the dissipation rate was very slow and had mostly stabilized, as the dye concentration lessened within the plot only 2.0 µg L^{-1} over this period (Fig. 2b).

South Plot

The initial whole plot RWT dye concentration collected from the handheld fluorometer readings (N=7) in Keeney Cove South were 19.8 µg L^{-1} at 2 HAT and 12.11 µg L^{-1} by 9 HAT (Fig. 2c). While these values were higher than the target concentration of 10 µg L^{-1}, the dye did not persist at these levels as the RWT concentration within the plot measured only 1.72 µg L^{-1} by 26 HAT (Fig. 2c). Rapid mixing occurred within Kenney Cove South as RWT dye measurements vertically equilibrated within the water column at 2 HAT (P=0.54; Fig. 3c), and no difference was detected between surface and bottom measures at any additional

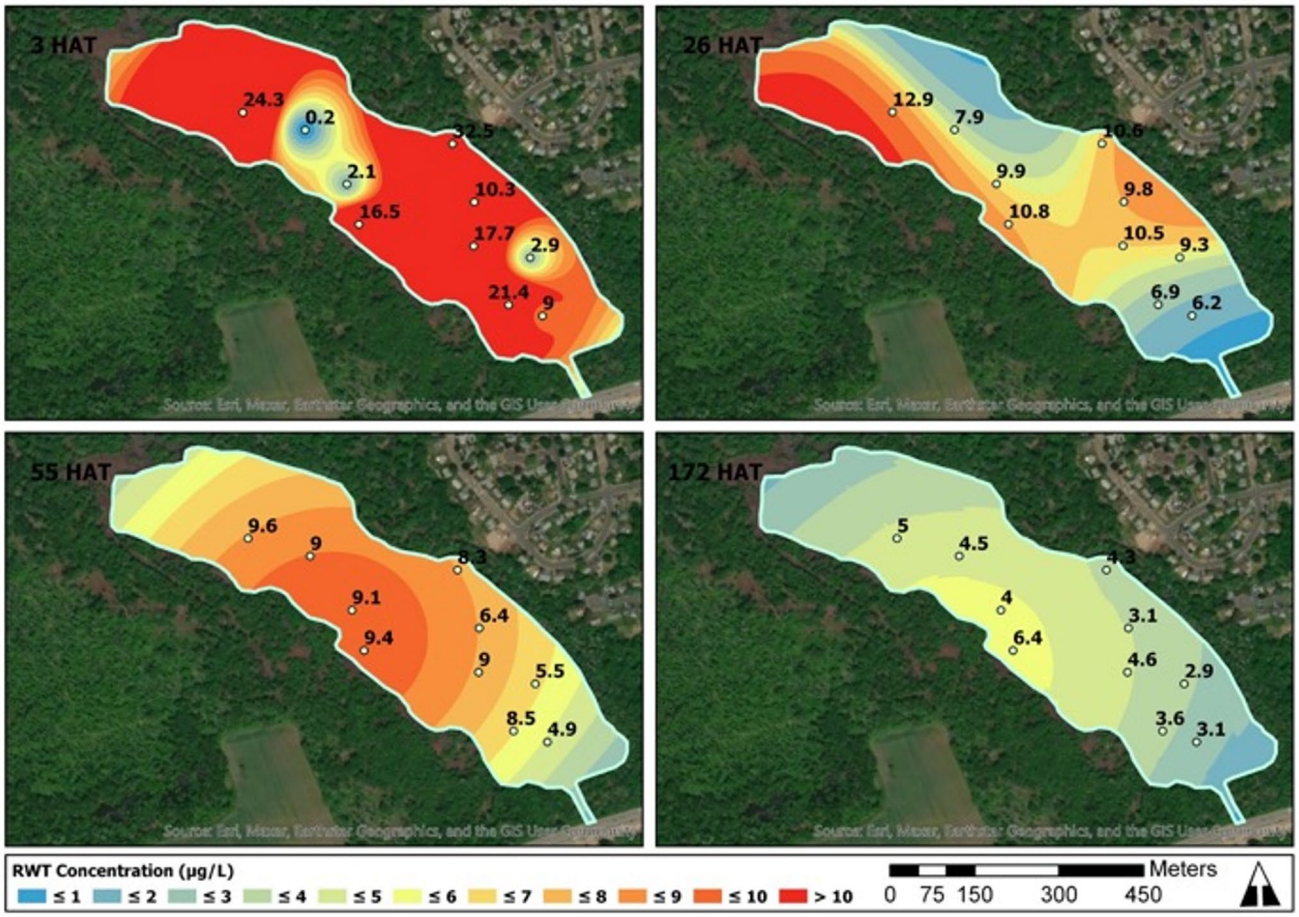

Fig. 4 Rhodamine (RWT) dye dissipation modeling in the Keeney Cove north plot from select time points having a target dye concentration of 10 µg L^{-1}. Individual points represent the mean water column dye concentration measured with a handheld fluorometer, while the gradient color scheme represents interpolated dye concentrations within the plot

dye samplings periods ($P > 0.05$). The estimated half-life in the South plot was the shortest in Keeney Cove at 9.96 h, which was 7.1 and 62.4 h less than the estimated half-life at the Keeney Cove Middle and North plots, respectively (Fig. 2). As anticipated, the closer proximity to the Lower CR channel prominently influenced the faster water exchange rates measured in Keeney Cove South (Fig. 6). These rapid dissipation trends were evident in the deployable sonde data ($N = 1$) also, as dye concentration peaked at 21.57 µg L^{-1} at 3 HAT but was not detected (0 µg L^{-1}) by 11 HAT at the sonde location (placed in creek channel) due to more rapid water exchange (Fig. S6). However, dye was redetected at 20 HAT but persisted for only 3 h at a mean concentration of 0.75 µg L^{-1}. This tidally influenced pulsing and dissipation pattern (i.e., frequency of low dye concentration and subsequent removal) occurred until sonde removal at 128 HAT.

Portland Boat Works

The initial whole plot RWT dye concentration collected from the handheld fluorometer readings ($N = 10$) at Portland Boat Works was 12.88 µg L^{-1} immediately following the dye application (i.e., 0 HAT) (Fig. 7a). This dye concentration was very close (SE ± 3.6) to the intended target concentration of 10 µg L^{-1} demonstrating that water volume conditions due to tidal influx were closely predicted. Dye measurements had vertically equilibrated within 0.25 HAT indicating rapid mixing occurred (Fig. 3d), as no difference was detected between surface and bottom measures following the initial sampling ($P > 0.05$). Portland Boat Works had the fastest water exchange measured of all the Lower CR sites evaluated, having an estimated half-life of 0.35 h (Fig. 7a). This rapid water exchange was not surprising considering the location of Portland Boat Works directly positioned

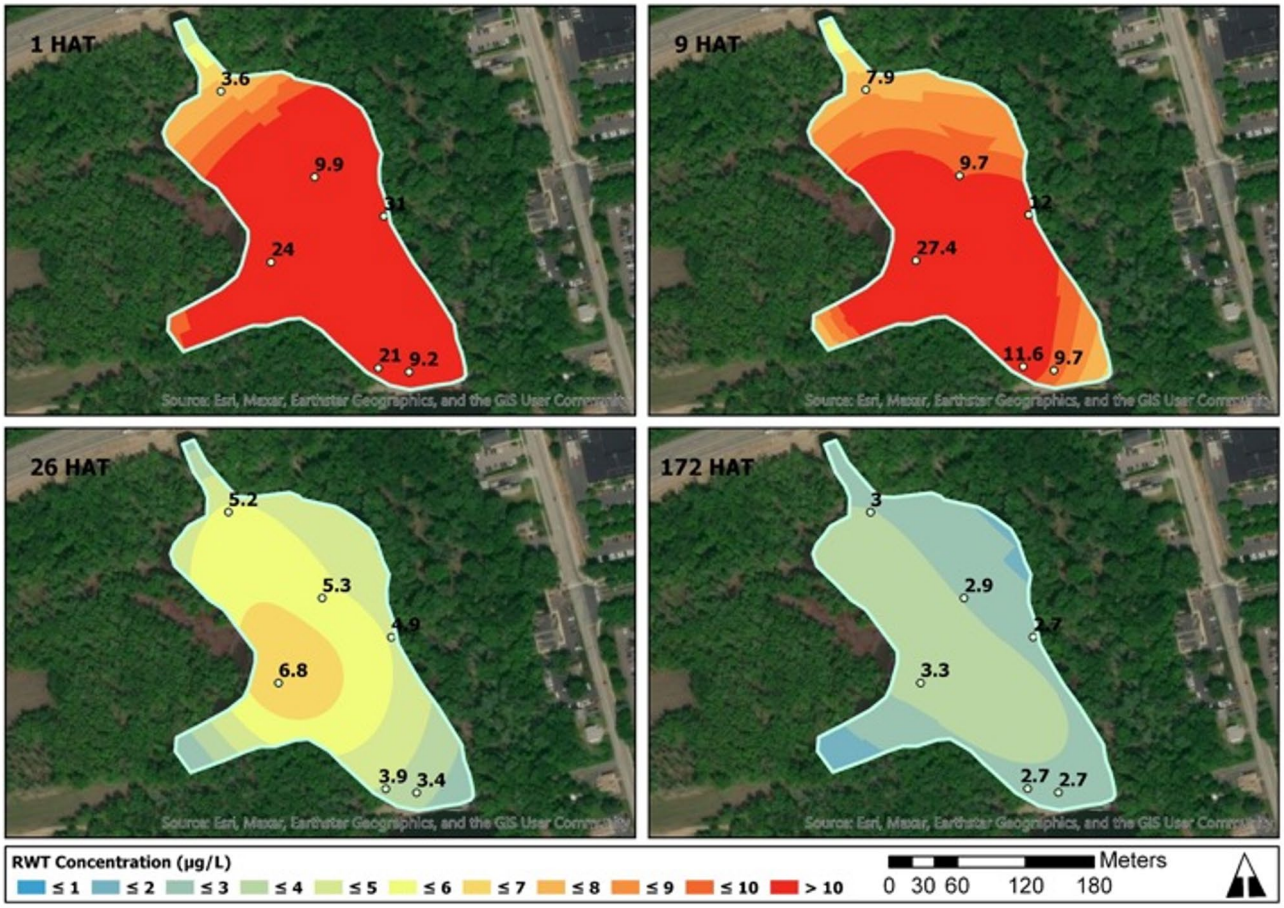

Fig. 5 Rhodamine (RWT) dye dissipation modeling in the Keeney Cove middle plot from select time points having a target dye concentration of 10 µg L^{-1}. Individual points represent the mean water column dye concentration measured with a handheld fluorometer, while the gradient color scheme represents interpolated dye concentrations within the plot

on a meandering portion of the Lower CR shoreline (Fig. 1). By 1 HAT, handheld fluorometer samplings showed the whole plot RWT dye concentration dissipated to 1.39 µg L^{-1}, and the dye was below detectable limits by 6 HAT (Figs. 7a). The deployable sondes ($N=3$) mimicked the dissipation pattern captured with the hand fluorometer, with dye values occurring below detectable limits at 0.67, 1.67, and 2.17 HAT (sonde 1, 3, and 4, respectively) (Fig. S7). The deployable sonde data and mapping elements further show the plot experienced a horizontal dye concentration gradient having a west-to-east heading, which directly corresponds to the direction of the CR flow (Fig. 8). Although the RWT dye within the plot was uniformly applied, dissipation patterns from 0 to 2 HAT illustrate the dye quickly accumulated along the shoreline where dye maintained the highest concentration within an eddy formed in the northeast corner of the marina.

Chapman Pond

The initial whole plot RWT dye concentration collected from the handheld fluorometer readings ($N=23$) at Chapman Pond was 16.9 µg L^{-1} at 0.5 HAT, with no dye detected outside of the treatment plot at this sampling (Figs. 7b and 9). Dye measurements were vertically equilibrated within 0.5 HAT (Fig. 3e), and no difference was detected between surface and bottom measures following initial dye readings ($P>0.05$). The whole plot half-life was estimated at 18.17 h (Fig. 7b), which closely matches the water exchange dynamics experienced at the Keeney Cove middle plot (17.03 µg L^{-1}) (Fig. 2b). Based on the handheld fluorometer and deployable sonde ($N=4$) data, RWT dye persisted at low-level concentrations (<5 µg L^{-1}) within the plot beyond 28 HAT recordings (Figs. 7b and S8). Distinct tidal fluctuation patterns captured with the deployable sondes suggest

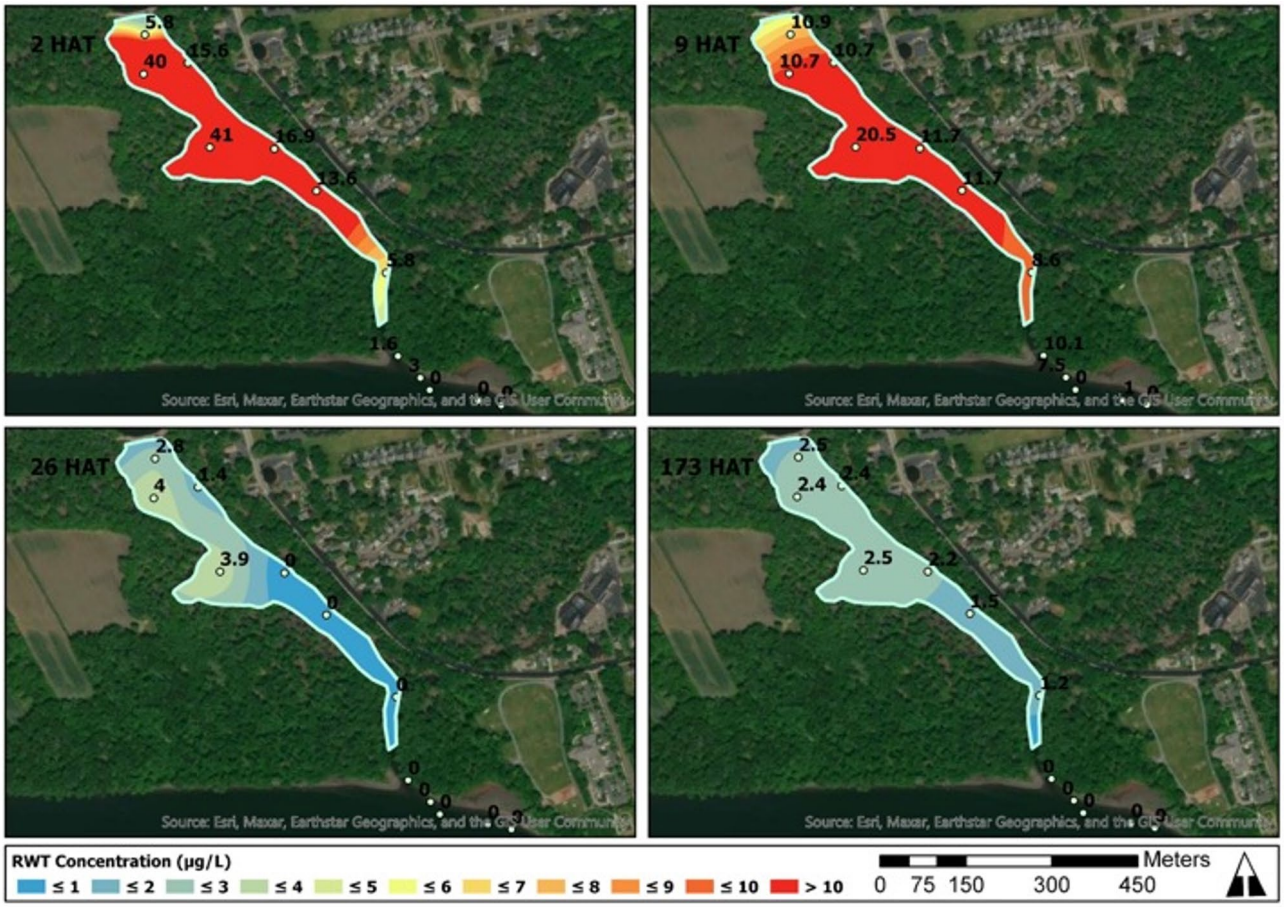

Fig. 6 Rhodamine (RWT) dye dissipation modeling in the Keeney Cove south plot from select time points having a target dye concentration of 10 µg L^{-1}. Individual points represent the mean water column dye concentration measured with a handheld fluorometer, while the gradient color scheme represents interpolated dye concentrations within the plot

Chapman Pond experienced prominent water exchange with each tide cycle as evidenced by each intermittent pulsing event (Fig. S8). The deployable sondes anchored towards the northern and southern extremes of the plot (sondes 3 and 4, respectively) showed those respective portions of the plot had the greatest RWT dye retention but also experienced the highest variance in dye concentration (Figs. 9 and S3). Both of these two deployable sondes were placed in portions of the pond heavily occupied with hydrilla (100% biovolume), whereas the other two deployable sondes were placed near the inlet (sonde 1) or deep portions of the pond (sonde 2). These dissipation patterns suggest higher dye retention occurred in areas where hydrilla growth was at or near the water's surface and therefore less affected by tidal regimes. Dissipation maps further support these water exchange trends, with the RWT dye persisting in shallower areas of the pond completely occupied by hydrilla (Table 1; Fig. 9). Rhodamine WT dye was detected in all sampling periods beyond 7.25 HAT on both the inlet and outlet portions of the pond, with the highest recordings befalling with outgoing tides on the outlet side (Fig. 9).

Chester Boat Basin

The initial whole plot RWT dye concentration collected from the handheld fluorometer readings ($N=36$) at Chester Boat Basin was 18.55 µg L^{-1} at 0.5 HAT and remained at equivalent levels at 4.5 HAT (18.17 µg L^{-1}) (Fig. 7c). A field-based volumetric calculation error led to an application rate of RWT dye that exceeded the intended 10 µg L^{-1} concentration; however, this did not affect the ability to evaluate water exchange and relative half-lives within Chester Boat Basin. Dye measurements captured at 0.5 and 4.5 HAT revealed whole plot differences ($P<0.0001$) between surface and bottom RWT dye concentrations (Fig. 3f), where the surface of the water column had 5.7- and 3.7-fold more RWT dye than the bottom measurements (0.5 and 4.5 HAT, respectively). However, whole water column vertical equilibration was achieved by 17.5 HAT ($P=0.756$) (Fig. 3f). The whole plot half-life estimate for Chester Boat Basin was 22.67 h (Fig. 7c), which was a longer RWT dye residency period than anticipated given the proximity of Chester Boat Basin to the main CR channel (Figs. 1 and S4). Deployable

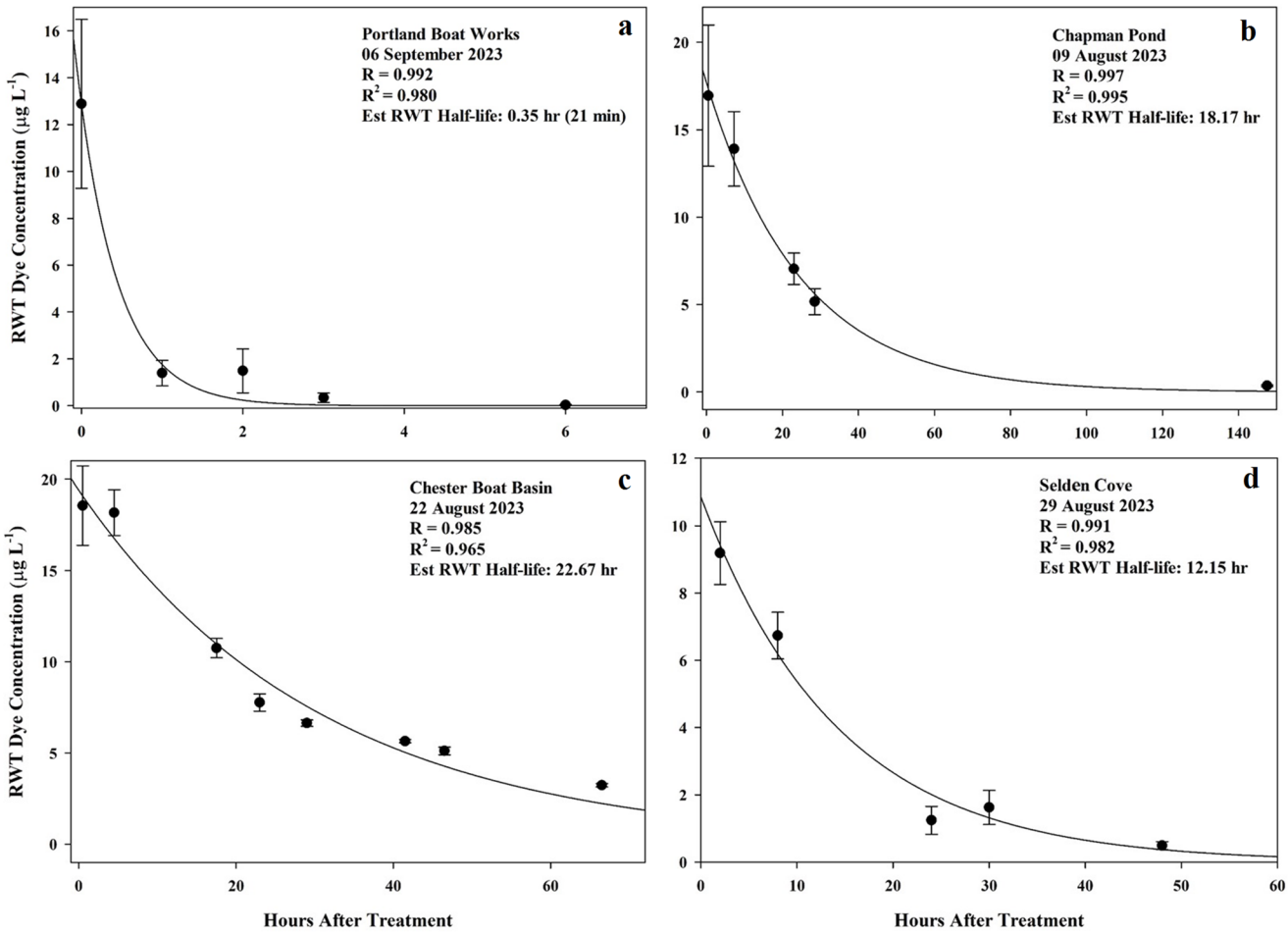

Fig. 7 Rhodamine (RWT) dye concentrations within the (**a**) Portland Boat Works; (**b**) Chester Boat Basin; (**c**) Chapman Pond; and (**d**) Selden Cove study plots over time measured with a handheld fluorometer. Data points represent the mean water column RWT concentrations (±SE) for each measured time point. Half-lives estimated using the exponential decay model, f=a*exp(-b*x)

sonde (N=4) data showed similar water exchange pulsing patterns as witnessed in Chapman Pond, where tidal cycles tightly compared to the handheld fluorometer measurements of RWT dye in the plot (Fig. S9). The deployable sondes also indicated that the edges and terminal ends of the cove (sondes 2 and 4) generally experienced greater and more extended RWT dye concentrations than sondes placed near the middle of the channel (sondes 1 and 3) (Fig. S4 and S9). Rhodamine dye dissipation mapping supports the observation that a greater concentration gradient occurred along the shoreline and terminal points of Chester Boat Basin over time (Fig. 10).

Selden Cove

The initial whole plot RWT dye concentration collected from the handheld fluorometer readings (N=17) at Selden Cove were 9.2 µg L^{-1} at 2 HAT and 6.73 µg L^{-1} by 8 HAT, which narrowly aligned (SE ± 0.93 and 0.69 µg L^{-1}, respectively) with the target concentration of 10 µg L^{-1} (Fig. 7d). However, the initial dye measurements at 2 HAT showed differences (P=0.0014) between surface and bottom RWT concentration measures (5.3 µg L^{-1} greater at surface), but vertical equilibration was achieved by 8 HAT (P=0.928) (Fig. 3g). The whole plot half-life was estimated at 12.15 h (Fig. 7d), which compares to intermediate half-life estimates between Keeney Cove South (9.96 µg L^{-1}) and Chapman Pond (18.17 µg L^{-1}) plots (Figs. 3c and 7b). At 24 HAT, handheld fluorometer readings indicated a whole plot RWT dye concertation of 1.24 µg L^{-1}, and by 48 HAT the majority of RWT dye had completely dissipated from the plot (<1.0 µg L^{-1}) (Fig. 11). Data collected with the deployable sondes (N=2) indicated Selden Cove experienced distinct intermittent pulsing of RWT dye (i.e., concentration pauses) at approx. 7 (1.36 µg L^{-1}), 14 (0.48 µg L^{-1}), and 23 (0.57 µg L^{-1}) HAT which, roughly corresponds to semidiurnal tide fluctuation intervals (Fig. S10). The Selden Cove plot was heavily infested with hydrilla

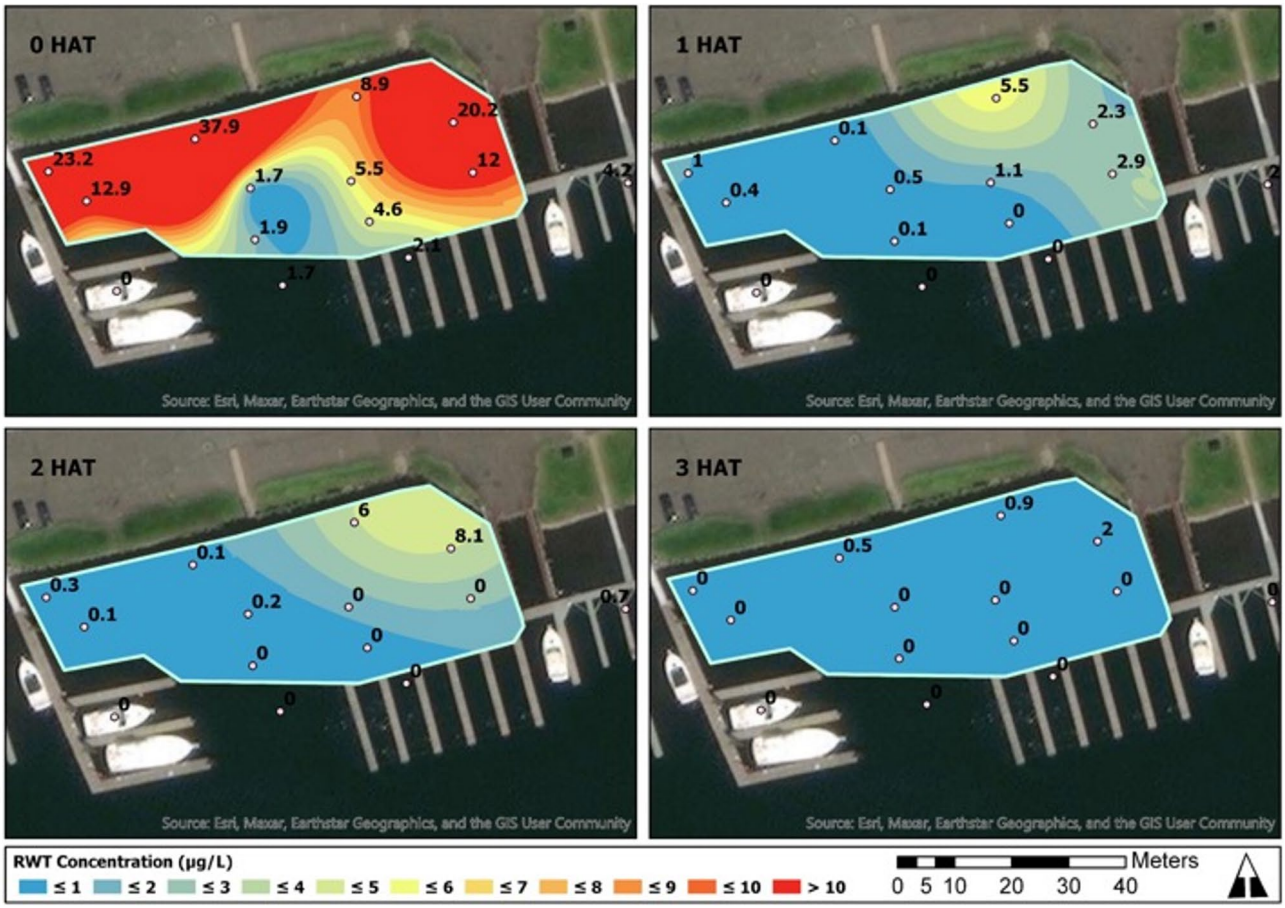

Fig. 8 Rhodamine (RWT) dye dissipation modeling in the Portland Boat Works plot from select time points having a target dye concentration of 10 µg L^{-1}. Individual points represent the mean water column dye concentration measured with a handheld fluorometer, while the gradient color scheme represents interpolated dye concentrations within the plot

(Table 1), and areas of the plot that were denser (towards the North end of the plot) maintained the longest RWT dye concentrations over time (Fig. 11). At each of the handheld fluorometer sampling periods, a minute quantity ($\mu < 1.0$ µg L^{-1}) of RWT dye was detected outside of the treatment plot (Fig. 11). However, these low RWT dye concentration values outside the plot accounted for <1.5% of the initial in-plot concentration (i.e., <0.15 µg L^{-1}) and suggests any dye lost from the treatment plot experiences rapid dilution upon release from Selden Cove given its proximity to the main river channel.

Discussion

Keeney Cove had the most unique water exchange characteristics following the assessments of three distinct cove sections (North, Middle, and South plots). The North plot of Keeney Cove was the furthest plot from the main Lower CR channel, had the highest density of vegetation, and displayed the longest half-life (72.36 h) of all studies. A study investigating invasive SAV control in a run-of-the-river reservoir suggested dense plant canopies notably increased RWT dye and herbicide residence time by slowing water exchange rates (Wersal et al., 2022) which, was also observed in the Keeney Cove North plot where dense hydrilla and water chestnut (*Trapa natans* L.) within the plot decreased water flow, resulting in an increased dye residency (Table 1). The North plot was additionally restricted via a bridge culvert on the inlet side (southernmost portion of the plot), which likely further delayed water exchange rates influenced via tide fluctuations. Keeney Cove's Middle plot was a transition zone between the impounded North plot and the South plot that behaved as the mouth of Keeney Cove to the Lower CR. The Middle Keeney Cove plot, having a pseudo inlet and outlet, displayed similar water exchange patterns (17.03 h half-life) as the ponded sites (Chapman Pond and Selden Cove). Like the North plot, the Middle plot was heavily vegetated with hydrilla and water chestnut (Table 1), particularly on the western plot edges where water depth was most shallow (Fig. S1). Since the Middle plot was situated between the CT Route 3 bridge

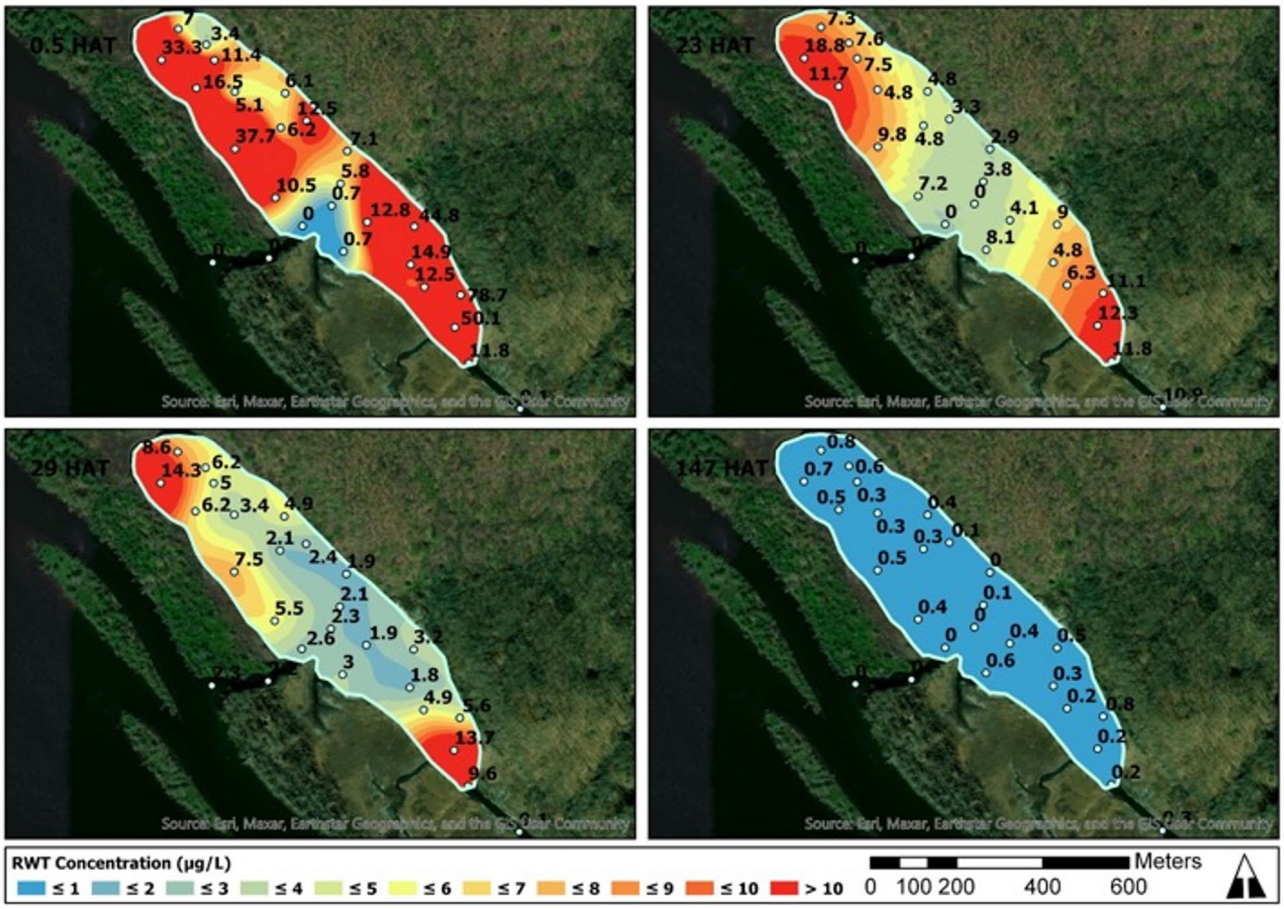

Fig. 9 Rhodamine (RWT) dye dissipation modeling in the Chapman Pond plot from select time points having a target dye concentration of 10 µg L^{-1}. Individual points represent the mean water column dye concentration measured with a handheld fluorometer, while the gradient color scheme represents interpolated dye concentrations within the plot

culvert (northernmost portion of the plot) and the Point Rd. bridge culvert (southernmost portion of the plot) (Fig. S1), these physical restriction zones likely further contributed to slowing water exchange rates. The half-life at Keeney Cove South (9.96 h) was unlike any of the other evaluation sites, and experienced water exchange 1.7- and 7.3-fold faster than the Middle and North Keeney Cove plots, respectively. Because Keeney Cove South was the last plot before adjoining the Lower CR, RWT dye was periodically captured over time with water exchange from the Middle and North plots with ebb tides after initial flushing. The most likely explanation for dye persistence, or repeated reappearance, over time in Keeney Cove South could be due to the upstream dye applications discharging from the Keeney Cove Middle and North treatment plots with each outgoing tide. Since RWT dye was detected leaving the South plot and lost to the main CR channel at both the 2 and 9 HAT samplings, with no dye measured outside the plot beyond 9 HAT (Fig. 6), dye reentry from the head of the cove is the most plausible explanation to this water exchange phenomenon. The Keeney Cove site provides evidence that sites having varying flow restriction points, or are subject to varying flow constants due to tidal influence or tributary, require segmentation to most accurately target intended CETs.

Apart from Selden Cove, all initial (0 to 3 HAT) handheld fluorometer readings indicated whole plot average RWT dye concentrations at 129 to 198% above the 10 µg L^{-1} target threshold. This implies that mixing of applied chemical solutions, such as RWT dye or herbicide, in the water-column are not immediate processes and exemplifies the importance of site-specific water exchange modeling to realize the associated complexities of vertical and horizontal mixing components due to SAV, bathymetry, and tidal flux. In the case of Selden Cove, presence of dense, surface matted hydrilla and a tidal flat ultimately limited uniform mixing initially and the ebb current from Selden Creek likely led to even more rapid diffusion of RWT dye from the plot. On the contrary, plots with higher initial concentrations (measured within 3 HAT) should be expected when applying a dye solution at predicted water volumes, since dye concentrations were calculated for incoming high-tide water volumes. Thus, the expectation of chemical thresholds as

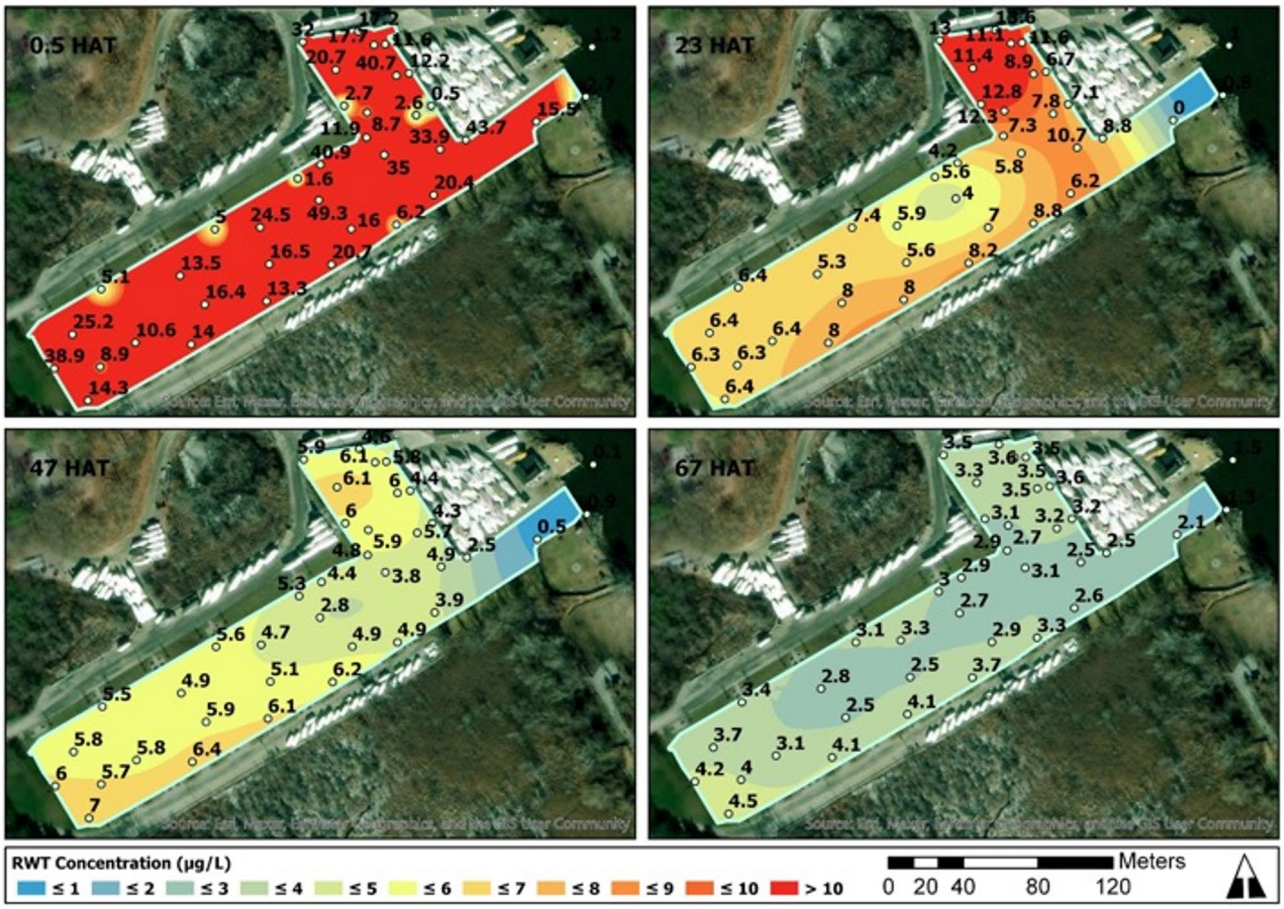

Fig. 10 Rhodamine (RWT) dye dissipation modeling in the Chester Boat Basin plot from select time points having a target dye concentration of 10 µg L^{-1}. Individual points represent the mean water column dye concentration measured with a handheld fluorometer, while the gradient color scheme represents interpolated dye concentrations within the plot

an immediate static target are likely not feasible in tidally influenced systems as indicated by the RWT dye residency calculated in the present studies and acceptable leeway in application timing should be carefully cogitated to meet intended CET requirements. While initial RWT dye concentrations targeted 10 µg L^{-1}, all sites were below the RWT dye target threshold by 18 HAT and most sites achieved the intended concentration following one full tide cycle (approx. 12.5 h).

The present RWT dye studies demonstrated the Lower CR experiences a myriad of water exchange patterns, most likely influenced by the study site's proximity to the main river channel, construction (e.g., cove or pond), vegetation density (i.e., biovolume), bathymetric composition, water flow and direction, and tide cycle interactions. Ponded sites having an inlet and outlet, like Chapman Pond and Selden Cove, displayed moderate water retention times (18.17 and 12.15 h half-lives, respectively). Prior water exchange evaluations at Roanoke Rapids Reservoir, NC, showed the presence of dense hydrilla extended RWT dye residency and reduced mixing under a dam-controlled riverine setting (Sartain et al., 2023). However, the presence of dense hydrilla did not appear to solely influence dye retention in Chapman Pond and Selden Cove. Additional environmental characteristics, such as bathymetric contour and channeling through the middle of the plot appeared to dictate the tidally influenced water exchange as alluded in prior studies (Fox et al., 1991a, b; Getsinger & Netherland, 2018).

Water exchange at Chester Boat Basin showed similar patterns to the ponded sites but the open channel that behaved as both an inlet and outlet (depending on the tide cycle) likely contributed to the slightly longer half-life observed (22.67 h). Prior investigations of tidally influenced water exchange at Crystal River, FL also showed greater dye concentrations towards the heads of the canals rather than the mouth (Fox et al. 1991a, b). Interestingly, RWT dye was measured leaving the treatment plot irrespective of the tide cycle at Chester Boat Basin, and dye concentration appeared to gradually increase in a clockwise pattern beginning at the southern shoreline edge of the plot (Fig. 10). Fox et al. (1991a, b) described a similar clockwise water exchange pattern due to thermal stratification from

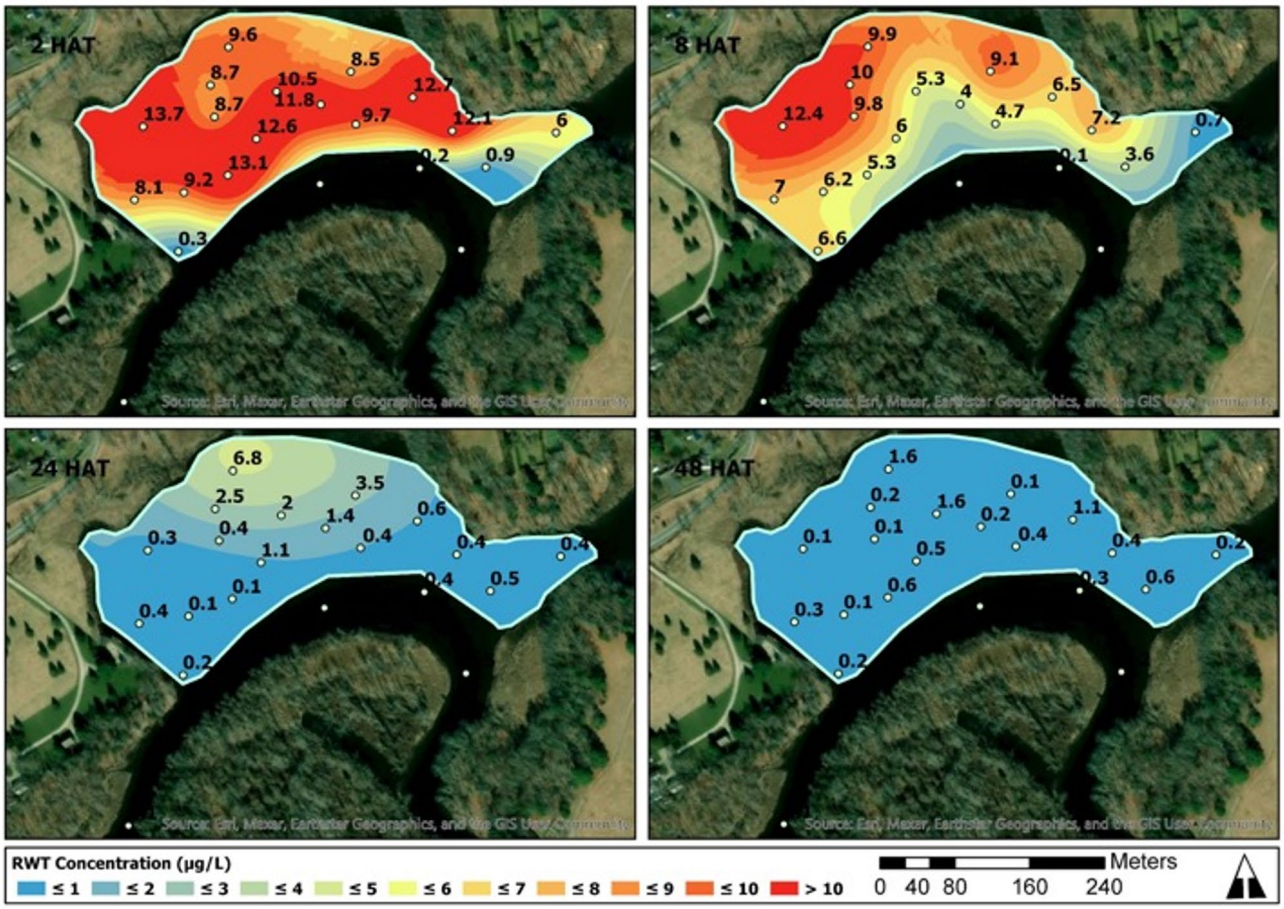

Fig. 11 Rhodamine (RWT) dye dissipation modeling in the Selden Cove plot from select time points having a target dye concentration of 10 µg L^{-1}. Individual points represent the mean water column dye concentration measured with a handheld fluorometer, while the gradient color scheme represents interpolated dye concentrations within the plot

an ebb tide where existing dye-treated surface water (warm water) exits while dense bottom water (cooler water) enters the canal. However, routine temperature measures did not identify thermal stratification at Chester Boat Basin, as the difference between the bottom and surface waters was typically ≤ 1.1 °C. Due to the narrow canal opening adjoining the main CR channel, additional water exchange processes likely occur, such as the Venturi effect (Sickbert & Peterson, 2014), which could have further implications on the dissipation patterns within Chester Boat Basin.

Shoreline locations along meandering portions of the Lower CR, like Portland Boat Works, had an extremely rapid water exchange (0.35 h half-life) in comparison to those sites of ponded of canaled morphology. A similar RWT dye study in the Potomac River, MD/VA discovered the presence of a dense hydrilla stand along the main river channel slowed flow velocities by approx. 10 times that of the unvegetated channel due to frictional forces (Rybicki et al., 1997). Even with reduced flow within the hydrilla inundated water column of Portland Boat Works, the western half of the plot dissipated to < 1 µg L^{-1} by 1 HAT (Fig. 8), which suggests additional application methods should be considered to improve RWT dye residency within the plot (e.g., sequential or drip herbicide applications). In riverine settings like those of Portland Boat Works, fully occupied SAV water columns can also experience an 'edge effect' created when aqueous solution concentrations applied in long, narrow plots dilute quicker than aqueous solutions applied to wider, more square plots due to reduced edge length exposure to diffusion and friction gradients (Getsinger & Netherland, 2018). Additional research is needed to determine how plot shape and slack tide conditions together influence the optimal timing for applying treatments in hydrilla vegetated sites along the main river channel.

All sites evaluated were densely occupied with hydrilla and other native and invasive macrophytes (e.g., *T. natans*, *V. americana*, *C. demersum*, and *E. canadensis*). Water columns having dense, surface-level vegetation have been shown to frequently experience thermal stratification (i.e., warm water near the surface and cool water at the benthic layer) (Getsinger et al., 1990); however, the present studies did not observe distinct differences in water column

temperatures. One possible explanation involves the main CR water temperature during the summer months (22 to 25 °C) with the semidiurnal tidal pattern, which theoretically mixes replacement water at approx. 6 h intervals at isothermal temperatures to the study sites. This likely corresponds to the vertical equilibration in dye concentration given the seasonal timing of the study (warmer water source in late summer). Another possibility is the relatively shallow bathymetric profiles ($\mu = 0.74$ to 1.93 m depths) within the study sites in combination with abundant SAV limited inundation of flood tide.

Tidal and hydrodynamic influences often negatively impact CET due to the rapid movement of water out of target management areas. The rapid exchange of water typically observed in most tidal systems reduces the potential exposure time, requiring new application methods to ensure effective management of invasive and noxious weeds. Netherland (2015) determined that continuous exposures of the aquatic herbicide, fluridone, may not be required for efficacious management including the introduction of "rest periods" between applications. Similarly, further examination of intermittent herbicide applications has revealed that discontinuous exposures do not significantly reduce the efficacious potential of the aquatic herbicide, endothall (Darnell, 2022; Beets et al., 2024). The concept of intermittent applications may reveal a technique to achieve more consistent herbicide efficacy in hydrodynamic systems. Intermittent applications in a tidal situation could be utilized to maximize CET and target applications during slack tides, with corresponding "rest periods" during flood/rising and ebbing tides.

Because of the associated negative effects hydrilla and other AIS poses within the Lower CR ecosystem, these site-specific evaluations and models provide an important guide for initiating chemical management strategies to reduce the deleterious effects of invasive species to improve water resource resilience. It should be noted that concern of downstream, off-site movement following chemical application (i.e., herbicide treatment) is limited based on the present findings (e.g., < 1.0 µg L^{-1} RWT dye detected outside of Selden Cove), and non-target risk could be further reduced using buffers or mitigation zones for sensitive flora adjacent to the downstream portions of channeled coves. Additional hydrilla infestation sites (e.g., Salmon Cove, Lower CR) may follow similar water exchanges as those presented in the present studies; however, confirmation of actual flushing rates should be applied independently to future management supported areas to ensure target CETs are met.

Summary and Management Implications

Site-specific water exchange patterns identified in the present studies need to be considered when developing herbicide-oriented hydrilla management programs in tidally-influenced riverine sites. Considering the vast ranges in bulk water exchange, study site proximity to the river channel, distance up-river, bathymetry, and vegetation density are all likely factors which ultimately dictate an applied solutions residency time in situ. Findings from our research are intended to guide initial chemical management operations based on unique herbicide CET requirements for hydrilla control.

- A need exists to evaluate small-scale herbicide CET studies to target hydrilla under simulated tidal influences (i.e., intermittent pulsing) to better understand the influence of this unique CET relationship.
- As more hydrilla management zones are identified along the Lower CR, additional water exchange evaluations based upon seasonality are needed to validate those CET relationships in comparison to the present studies.
- Contrasts of RWT dye and herbicide applied simultaneously under field-studies would improve the current understanding of site-specific water exchange patterns since herbicides are more prone to adsorption and faster degradation pathways compared to RWT dye.
- Water quality parameters (e.g., ph, temperature, DO, turbidity) should be carefully considered when selecting herbicides for hydrilla management programs regarding individual tidally influenced water exchange patterns of the Lower CR due to varying herbicide environmental fates and degradation pathways (e.g., diquat readily binds to suspended solids, thus limiting invasive plant adsorption of the chemical in highly turbid waters).
- Among management sites having relative long half-lives (> 18 h), slower-acting herbicides (e.g., florpyrauxifen-benzyl) or lower rates of fast-acting herbicides (e.g., endothall) could be used due to increased residency periods.
- Control of hydrilla, or other invasive aquatic species, within management sites having relatively short half-lives (< 12 h) would benefit from fast-acting herbicide applications (e.g., endothall, diquat, or combinations of both) applied with weighted drop hoses or a controlled delivery metered injection system.

Acknowledgements The authors would like to thank Keith Hannon, Ben Lloyd, Sean Terrill, Hannah Doherty, and Donnie Faughnan at the USACE New England District for project management and technical assistance; Marc Bellaud and Keith Gazaille at Solitude for dye application and field assistance; and Greg Bugbee, Jeremiah Foley, Riley Doherty, and Summer Stebbins at the Connecticut Agricultural Experiment Station for technical support. Permission was granted by the Chief of Engineers to publish this information. Citation of trade names does not constitute endorsement or approval of the use of such commercial products.

Financial Interests The authors declare they have no financial interests.

Authors' Contributions Conceptualization: AWH, BPS, MWD, JSG; methodology: AWH, BPS, MWD, JSG; data acquisition and management: AWH, BPS, MWD, JSG, AER; supervision: BPS; formal analysis and investigation: AWH; MWD; writing and editing original draft preparation: AWH, BPS, JPB; funding acquisition: BPS. All authors have read and approved the final manuscript.

Funding This research was supported by the Aquatic Plant control Research Program at the U.S. Army Engineer Research and Development Center.

Data Availability The datasets during and/or analyzed during the current study available from the corresponding author on reasonable request.

Declarations

Ethics Approval and Consent to Participate Not applicable.

Consent for Publication Not applicable.

Competing Interests The authors declare that they have no competing interests.

References

Beets, J. P., Haug, E. J., Sperry, B. P., Thum, R. A., & Richardson, R. J. (2024). Response of four Vallisneria taxa to aquatic herbicides. *Invasive Plant Science and Management*. https://doi.org/10.1017/inp.2024.33

[CAES] Connecticut Agricultural Experiment Station (2020). Invasive Aquatic Plants in the Connecticut River. Accessed from: https://caes.maps.arcgis.com/apps/webappviewer/index.html?id=007f6ee203b74bcbb1d6e68a953d8baf

Clay, C., Deininger, M., Hafner, J., Adams, A., Faber, B., Shear, L. (2006) The Connecticut River watershed: Conserving the heart of New England. The Trust for Public Land, Boston, p. 56.

Darnell, T. L. (2022). Reproductive Biology and Management of Dioecious Hydrilla verticillata (L.f.) Royle. Master's thesis. [Gainesville]: University of Florida. 132 p.

Foley IV, J. R., Stebbins, S. E., Doherty, R., Tippery, N. P., Bugbee, G. J. (2024) Northern hydrilla(Hydrilla verticillata ssp. lithuanica): discovery and establishment outside the Connecticut River. *Invasive Plant Science and Management, 17*(1),55–59.

Fox, A. M., Haller, W. T., & Getsinger, K. D. (1991b). Factors that influence water exchange in spring-fed tidal canals. *Estuaries*, *14*(4), 404–413.

Fox, A. M., & Haller, W. T. (1992). Improving herbicide efficacy in spring-fed tidal canals by timing and application methods. *Journal of Aquatic Plant Management, 30*, 58–62.

Fox, A. M., Haller, W. T., Getsinger, K. D., & Green, W. R. (1991a). Characterization of Water Movement in Hydrilla-Infested Tidal Canals of the Crystal River, Florida. MP A-91-2. Vicksburg, MS: US Army Engineer Waterways Experiment Station. https://apps.dtic.mil/sti/pdfs/ADA235669.pdf

Getsinger, K. D., Fox, A. M., & Haller, W. T. (1990). *Understanding water exchange characteristics to improve the control of submersed plants. Aquatic plant control research program: Information exchange bulletin*. US Army Engineer Research and Development Center. Environmental Laboratory A-90-2.

Getsinger, K. D., & Netherland, M. D. (2018). Use of herbicides in areas of high water exchange: Practical considerations. *J Aquat Plant Manage*, *56s*, 39–43.

Getsinger, K. D., Mudge, C. R., Sartain, B. T., Sperry, B. P., Walter, D. J., & Durham, M. W. (2024). The use of rhodamine water tracer (RWT) dye to improve submersed herbicide applications. ERD/EL SR-24-4. 24 pp.

Haller, W. T. (1982). Hydrilla goes to Washington. *Aquatics*, *4*(4), 6–7.

Haller, W. T., Shiremana, J. V., & Duranta, D. F. (1980). Fish harvest resulting from mechanical control of hydrilla. *Transactions of the American Fisheries Society, 109*(5), 517–520.

Hofstra, D., Champion, P., & Clayton, J., (2010) Predicting invasive success of Hydrilla verticillata (Lf) Royle in flowing water. *Hydrobiologia, 656*(1), 213–219.

Jacono, C. C., Richerson, M. M., Howard Morgan, V., Pfingsten, I. A., & Redinger, J. (2025). Hydrilla verticillata (L. f.) Royle: U.S. Geological Survey, Nonindigenous Aquatic Species Database, Gainesville, FL. https://nas.er.usgs.gov/queries/FactSheet.aspx?SpeciesID=6, Revision Date: 8/8/2024, Peer Review Date: 10/27/2015, Access Date: 2/18/2025.

Jones, C. G., Lawton, J. H., & Shachak, M. (1997). Positive and negative effects of organisms as physical ecosystems engineers. *Ecology, 78*, 1946–1957.

Langeland, K. A. (1996). *Hydrilla verticillata* (L.f.) Royle (Hydrocharitaceae), "the perfect aquatic weed." *Castanea, 61*, 293–304.

Madsen, T. V., & Sand-Jensen, K. (1991). Photosynthetic carbon assimilation in aquatic macrophytes. *Aquatic Botany*, *41*, 5–40.

Moore, H. H., Niering, W. A., Marsicano, L. J., & Dowdell, M. (1999) Vegetation change in created emergent wetlands (1988-1996) in Connecticut (USA). *Wetlands Ecology and Management, 7*(4),177–191.

Moore, K. A., Shields, E. C., & Jarvis, J. C. (2010). The role of habitat and herbivory on the restoration of tidal freshwater submerged aquatic vegetation populations. *Restoration Ecology, 18*, 596–604.

Netherland, M. D., & Getsinger (1992). Efficacy of Triclopyr on Eurasian watermilfoil: Concentration and exposure time effects. *J Aquat Plant Manage*, *30*, 1–5.

Netherland, M. D. (1997) Turion ecology of hydrilla. *Journal of Aquatic Plant Management, 35,* 1–10.

[NMFS] National Marine Fisheries Service (2024). Atlantic Sturgeon (*Acipenser oxyricnchus oxyrinchus*). Accessed 21 February 2025 from https://www.fisheries.noaa.gov/species/atlantic-sturgeon

Parker, B. B. (2007). *Tidal analysis and prediction. NOAA special publication NOS COOPS 3* (p. 378). U.S. Department of Commerce.

Runkel, R. L. (2015). On the use of rhodamine WT for the characterization of stream hydrodynamics and transient storage. *Water Resources Research, 51*, 6125–6142. https://doi.org/10.1002/2015WR017201

Rybicki, N. B., Jenter, H. L., Carter, V., Balzer, R. A., & Turtora, M. (1997). Observations of tidal flux between a submersed aquatic plant stand and the adjacent channel in the Potomac River near Washington, D.C. *Limnology and Oceanography, 42*(2), 307–317.

Sartain, B. T., Getsinger, K. D., Walter, D. J., Madsen, J. D., & Levoy, S. (2022). *Flowering rush control in hydrodynamic systems. Part 1: Water exchange processes*. US Army Engineer Research and Development Center, Environmental Laboratory.

Santos, M. J., Lars, W., Anderson, & Ustin, S. L. (2011). Effects of invasive species on plant communities: An example using submersed aquatic plants at the regional scale. *Biological Invasions*, *13*, 443–457.

Sartain, B. T., Haug, E. J., Getsinger, K. D., Sperry, B. P., Heilman, M. A., & Greer, M. (2023). *Small plot applications of Florpyrauxifen– benzyl (Procellacor SC™) for control of monoecious hydrilla in Roanoke rapids Lake, NC*. US Army Engineer Research and Development Center. https://doi.org/10.21079/11681/47115., Environmental Laboratory.

Savoy, T., Maceda, L., Roy, N. K., Peterson, D., & Wirgin, I. (2017). Evidence of natural reproduction of Atlantic sturgeon in the Connecticut river from unlikely sources. *PLoS One, 12*(4), e0175085.

Schmitz, D. C., Nelson, B. V., Nall, L. E., & Schardt, J. D. (1991). Exotic aquatic plants in Florida: A historical perspective and review of the present aquatic plant regulation program. pp. 303–326. In: T. C. Center, R. F. Doren, R. L. Hofstetter, R. L. Myers, L. D. Whiteaker (Eds.) Proceedings of the symposium on exotic plant pests. Technical report NPS/NREVER/ NRTR—91/06. National Park Service, United States Department of the Interior, Washington, DC.

Sickbert, T., & Peterson, E. (2014). The effects of surface water velocity on hyporheic interchange. *Journal of Water Resource and Protection*, *6*, 327–336. https://doi.org/10.4236/jwarp.2014.64035

Smart, R. M., Barko, J. W., & McFarland, D. G. (1994). Competition between Hydrilla verticillata and Vallisneria americana under different environmental conditions. Technical Report A-94-1, U.S. Army Engineer Waterways Experiment Station, Vicksburg, MS.

Stephens, N. E., Blackburn, R. D., Seaman, D. E., & Weldon, L. W. (1963). Flow retardance by channel weeds and their control. *Journal of the Irrigation and Drainage Division. ASCE, 89*, 31–47.

Steward, K. K., Van, T. K., Carter, V., & Pieterse, A. H. (1984). Hydrilla invades Washington, DC and the Potomac. *American Journal of Botany, 71*(1), 162–163.

Tippery, N. P., Bugbee, G. J., Stebbins, S. E. (2020) Evidence for a genetically distinct strain of introduced hydrilla verticillata (Hydrocharitaceae) in North America. *Journal of Aquatic Plant Management, 58*(1),1–6.

True-Meadows, S., Haug, E. J., & Richardson, R. J. (2016). Monoecious hydrilla—Areview of the literature. *J. Aquat. Plant Manage, 54*, 1–11.

Turner, E. G., Getsinger, K. D., & Netherland, M. D. (1994). Correlation of triclopyr and rhodamine WT dye dissipation in the Pend Oreille River. *Journal of Aquatic Plant Management, 32*, 39–41.

[USACE] U. S. Army Corps of Engineers. (2013). Engineering and Design: HYDROGRAPHIC SURVEYING. EM 1110-2-1003. Engineer Manual. 699 pg.

[USGS] U.S. Geologic Survey. 2024. Connecticut water conditions. Retrieved March 8, 2024, from https://waterdata.usgs.gov/ct/nwis/currentindex_pmcode_STATION_NM=1&index_pmcode_DATETIME=2&index_pmcode_00060=3&index_pmcode_MEAN=4&group_key=NONE&sitefile_output_format=xml&column_name=agency_cd&column_name=site_no&column_name=station_nm&format=html_table&sort_key_2=site_no&html_table_group_key=huc_cd&rdb_compression=file&list_of_search_criteria=realtime_parameter_selection

Weiss, L. A., Bingham, J. W., & Thomas, M. P. (1982). *Water resources inventory of Connecticut. Part 10: Lower Connecticut river Basin. Connecticut water resources commission bulletin No.31*. Connecticut Department of Environmental Protection.

Wersal, R. M., Sartain, B. T., Getsinger, K. D., Madsen, J. D., Skogerboe, J. G., Nawrocki, J. J., Richardson, R. J., & Sternberg, M. R. (2022). Improving chemical control of nonnative aquatic plants in run-of-the-river reservoirs. *Invasive Plant Science and Management, 15*, 141–151. https://doi.org/10.1017/inp.2022.18

Whitney, M. M., Jia, Y., Cole, K. L., MacDonald, D. G., & Huguenard, K. D. (2021). Freshwater composition and connectivity of the Connecticut River plume during ambient flood tides. *Frontiers in Marine Science, 8*, Article 747191. https://doi.org/10.3389/fmars.2021.747191

Williams, C. F., & Nelson, S. D. (2011). Comparison of Rhodamine-WT and bromide as a tracer for elucidating internal wetland flow dynamics. *Ecological Engineering*, *37*, 1492–1498. https://doi.org/10.1016/j.ecoleng.2011.05.003

Zhang, C., & Boyle, K. J. (2010). The effect of an aquatic invasive species (Eurasian watermilfoil) on lakefront property values. *Ecological Economics, 70*, 394–404. https://doi.org/10.1016/j.ecolecon.2010.09.011

Zhu, Z., Motta, D., Jackson, P. R., & Garcia, M. H. (2017). Numerical modeling of simultaneous tracer release and piscicide treatment for invasive species control in the Chicago sanitary and ship canal, Chicago, Illinois. *Environmental Fluid Mechanics*, *17*(2), 211–229. https://doi.org/10.1007/s10652-016-9464-1